EFFECTS OF HYDRAULIC LOADING ON NITRIFICATION AND DENITRIFICATION PROCESSES IN A TWO-STAGE, VERTICAL FLOW TREATMENT WETLAND AT BRIDGER BOWL SKI AREA

by

Robert Arthur Panighetti

A thesis submitted in partial fulfillment
of the requirement of the degree

of

Master of Science

in

Environmental Engineering

MONTANA STATE UNIVERSITY
Bozeman, MT

August 2020

ACKNOWLEDGEMENTS

I am extremely grateful to the numerous employees, faculty, and graduate students that were instrumental in conducting this research. In particular, I would like to thank Bridger Bowl, Inc., for continuing to support MSU and the treatment wetland project. Additionally, I would like to thank the members of my committee and many helpful assisting graduate students for their abundance of patience and guidance over the course of this project.

TABLE OF CONTENTS

LIST OF TABLES

Table Page

LIST OF FIGURES

Figure Page

LIST OF FIGURES - CONTINUED

Figure Page

LIST OF FIGURES - CONTINUED

Figure Page

ABSTRACT

A pilot-scale two-stage vertical flow treatment wetland (VFTW) at the Bridger Bowl Ski Area was used to evaluate the influence of hydraulic loading rate on COD removal, nitrification, and denitrification in the system. Hydraulic loading rates ranged between 36 cm/d to 60 cm/d over system years 2018 and 2019. Total nitrogen loading (sum of NH_4^+ and NO_3^-) ranged from 12 g/m^2d to 65 g/m^2d, and COD loading ranged from 58 g/m^2d to 172 g/m^2d. The system effectively removed COD in both years, with removals of 95% and 96% for influent COD concentrations of 555 mg/L and 607 mg/L, respectively. Influent total nitrogen was 141 mg/L in 2018 and 105 mg/L in 2019, and removals were 67% and 54%, respectively. At a hydraulic loading rate of 60 cm/d, COD removal declined in the first stage and ammonium removal declined in the second stage. At lower hydraulic loading rates (up to 48 cm/d), removal of COD, ammonium and nitrate increased in a consistent pattern with increased mass loading of the respective contaminant, suggesting a maximum hydraulic loading rate limit between 48 and 60 cm/d. The effect of hydraulic loading cannot be completely separated from mass loading of a contaminant, likely influenced by the level of partial saturation within the first stage and the recycle ratio; neither were varied in this study. A key limiting factor is hydraulic overload to the first stage, limiting removal of COD which interfered with nitrification in the second stage. A multivariate model for ammonium removal in the second stage predicts increased ammonium removal with increasing ammonium load but decreasing COD load. Despite operational performance variation the system met applicable discharge requirements, reinforcing the ability of a VFTW system to perform secondary wastewater treatment, even for high-strength wastewater and in cold climates.

INTRODUCTION

Constructed, or more specifically treatment wetlands (TW), offer a more natural solution for wastewater treatment, providing an attractive alternative to pond, land application and forced aeration systems. While the United States is slow to widely accept new water treatment technologies, TW are used in many European countries such as Austria, France, and Germany. TW are flexible systems that can be used for treatment of wastewaters with a variety of characteristics, such as acidic and metal-rich mine drainage, stormwater, runoff from agriculture or landfills, and domestic wastewater. They are often used for small communities (less than 1,000 people) or as an extra polishing step after a standard wastewater treatment system, and thus the upper applicability limits of the technology have yet to be seen (Luderitz et al., 2001).

Treatment wetlands, like conventional wastewater treatment systems, focus primarily on removal of organic carbon, nitrogen, and total suspended solids (TSS). Organic carbon and TSS indicate the level of organic contamination and toxicity of the wastewater, and if discharge reaches natural water sources, could lead to disease. Nitrogen contamination, after reaching a natural water source, can lead to eutrophication and reduced dissolved oxygen. This can cause mass death of aquatic life and reduced appeal for human recreation. In TW systems, removal of organic carbon and nitrogen occurs naturally by the microbial communities in the macrophyte rhizosphere, with the additional support of the media, which is also the primary filter for TSS removal. Organic carbon is removed by several heterotrophic processes depending on the redox status of the microsite within the wetland.

Nitrogen removal occurs primarily in two major processes: nitrification and denitrification. The balance between aerobic nitrification and anoxic denitrification forms the basis of TW system design and optimization when regulation requires nitrogen removal.

While treatment wetlands have many uses and designs, the three main designs for secondary wastewater treatment are vertical flow (VFTW), horizontal flow (HFTW), and free water surface (FWS), each with different advantages (Dotro et al., 2017). VFTW favor an aerobic subsurface, and thus nitrification, due to the periodic application of wastewater volumes, also referred to as doses, at the surface. Between wastewater doses, oxygen reenters the media pore space, maintaining an aerobic environment. The water is treated as it flows downward through the planted media and is typically drained from the bottom of the cell. The VFTW design excels at removal of organic carbon (via aerobic respiration) and ammonia nitrogen, with adjustments made through media choice and recirculation (Stefanakis et al., 2014). In contrast, HFTW favor an anaerobic subsurface, as water flows horizontally through the media, fully saturating it. HFTW systems generally favor denitrification, and thus struggle to remove ammonia, but are often used in hybrid systems in conjunction with other wetland designs, such as a VFTW, for more complete treatment (Vymazal, 2005). Unlike the VFTW and HFTW subsurface flow systems, FWS wetlands have a water level above the surface as well as a saturated root zone creating a vertical oxygen gradient. Thus, FWS wetlands have a less predictable mix of nitrification and denitrification, with the net effect depending largely on the choice of media and hydraulic loading rate. Due to the open water surface FWS wetlands risk

human exposure to wastewater contamination and are rarely used for secondary wastewater treatment (Kadlec and Wallace, 2009).

In fall 2012, Montana State University (MSU) supported the Montana Department of Environmental Quality (MDEQ) and Bridger Bowl, Inc. in construction of a VFTW system to enhance wastewater treatment at Bridger Bowl Ski Resort north of Bozeman, Montana. The system uses the preexisting septic tanks for primary treatment and replaced the recirculating sand filter with a VFTW for secondary treatment. The experimental, pilot-scale system consists of two stages with capabilities for recycle and variation of hydraulic loading rate and water depth to allow for maximum adaptability with a goal to improve understanding of VFTW capabilities to meet water quality standards set by MDEQ. The system has been in operation since December 2013, and a full-scale (four-times larger) system of identical design was constructed in summer 2018.

The Bridger Bowl TW design generally follows the new Danish guidelines for VFTW, allowing for results to be compared to similar systems (Arias and Brix, 2005). The wastewater treated is considered high strength, as it is mostly produced by kitchens and lavatories. Additionally, wastewater generation depends primarily on skier visits, resulting in significant wastewater flows for approximately one-third of the year when temperatures are coldest. These factors can be considered a stress test for comparison to a general VFTW, as similar systems with more typical environments and influent wastewater should perform better.

Since the system began operation in 2013, MSU researchers have shown that system performance regarding removal of BOD_5, COD, and TSS has been consistently good under a wide variety of operational parameters. Results in 2014-2015 determined

that small, frequent dose volumes allowed for superior COD removal averaging 91% (Moss, 2016). Still, maximum total nitrogen removal was 58%, suggesting a need for further optimization of nitrification and denitrification. Research in 2016-2017 focused on a greater variety of operational parameters, including saturation level, recirculation ratio, hydraulic loading rate, and dosing frequency (Woodhouse, 2018). These findings led to an average system removal of 95% for COD and 75% for total nitrogen in 2017 using a 2:1 recycle ratio, a 71 cm saturation depth, and twelve separate applications of septic water daily. Each application volume is identical and controlled by the active duration of the septic pump, creating the system doses. The present work used higher influent flow rates to attempt to find an upper limit for system performance.

Research objectives for the 2018 and 2019 seasons were a focused continuation of previous goals with additional focus on nitrogen dynamics within the system. Operating parameters remained consistent with those established in the 2017 season, and the influent flow rate was increased to values higher than previously tested. This would lead to discovery of the upper limits for nitrification and denitrification in the system by observing removals of COD, nitrate, and ammonium. Influent COD concentrations in 2018-2019 were also consistently lower than historical values, allowing for additional exploration of the differing effects caused by hydraulic loading and COD loading on the system.

This thesis is presented in several chapters. The literature review explores important processes and hydraulic effects on system performance for treatment wetlands. The methods section outlines procedures used for system operation, sample testing, and results analysis. Results and discussion follow, presenting the data collected in the 2018

and 2019 ski seasons and drawing relationships between factors controlling performance including comparisons with previously collected data when appropriate. The final section includes conclusions suggestions for future work.

LITERATURE REVIEW

Introduction

While often simplified to nitrification and denitrification, the processes influencing removal of nitrogen in a TW are complex and interrelated. The nitrogen cycle describes the biogeochemical transformations between various forms of nitrogen and is paramount to understanding the impact of different influent conditions on system performance. This literature review will describe the nitrogen transformation pathways relevant to a VFTW, analyze possible effects of increased hydraulic loading, and evaluate how these factors have impacted similar VFTW systems.

Mechanisms of Nitrogen Removal

Nitrogen removal in a constructed wetland occurs primarily through biological and physiochemical mechanisms. The biological methods use interactions between biofilms, which form on plant roots and surrounding media (rhizosphere), and the microbial communities in the wastewater. These methods include ammonification, anaerobic ammonia oxidation (ANAMMOX), nitrification, denitrification, and plant uptake (Lee et al., 2009). Biological transformations account for most of the nitrogen removal in a TW, and the predominant mechanism depends on the presence of dissolved oxygen and a carbon source, as well as the form of the nitrogen. The main physiochemical processes in a TW are ammonia volatilization, ammonia adsorption, and sedimentation (Vymazal, 2007). Many of these transformations are difficult to monitor and control, so emphasis is often placed on prioritization of nitrification or denitrification to allow for near complete nitrogen removal, forming the design basis for most TW.

Biological Nitrogen Transformation

Nitrogen transformation pathways allow for conversion between the different forms of nitrogen in wastewater. Organic nitrogen is present as a variety of compounds, such as proteins and amino acids, but most important for wastewater is urea. In standard domestic wastewater, urea can represent 80% of the total nitrogen (Hanson & Lee, 1971). As wastewater treatment progresses, inorganic nitrogen becomes predominant. Inorganic nitrogen is present as ammonium (NH_4^+), nitrite (NO_2^-), and nitrate (NO_3^-), as well as gaseous nitrogen as dinitrogen (N_2) (Vymazal, 2007).

Ammonification: The first nitrogen transformation that typically occurs in wastewater treatment is ammonification. For ammonification, the microbial community processes organic nitrogen into ammonia according to the following basic reaction:

$$Organic\ Nitrogen + Microorganisms \rightarrow Ammonia\ (NH_3/NH_4^+)$$

Ammonification is kinetically faster than nitrification, and occurs predominantly during primary treatment (Lee et al., 2009). The species of ammonia formed depends on the temperature and pH of the water. For domestic wastewater of typical pH, most of the ammonia is ionized into ammonium (NH_4^+). In most TW, ammonification is nearly complete before the wastewater enters the wetland, resulting in very little remaining organic nitrogen to be treated by the TW. Considering organic carbon and ammonia as the primary inputs allows system design to focus on nitrification and denitrification, the main processes responsible for nitrogen removal.

Nitrification: Nitrification is an aerobic process, requiring oxygen, ammonium, and a nitrifying autotrophic microbial community (Dotro et al., 2017). Nitrification

occurs over multiple steps, beginning with the oxidation of ammonia to nitrite. The nitrite is then further transformed in several steps to nitrate. This reaction pathway is simplified as follows:

$$NH_4^+ + 1.5O_2 \rightarrow 2H^+ + H_2O + NO_2^-$$

$$NO_2^- + 0.5O_2 \rightarrow NO_3^-$$

Both oxidation processes are performed by chemolithic autotrophic bacteria, with carbon dioxide as the carbon source, oxygen as the electron acceptor, and either ammonia or nitrite as the energy source (Lee et al., 2009). Nitrification also relies on the presence of alkalinity, mainly as $CaCO_3$, and rates decline at lower pH. The combination of proton production and consumption of alkalinity as a carbon source can lead to decreased wastewater pH, negatively impacting further nitrification, but this is typically insignificant in treatment wetlands. The specific bacteria are diverse, but common genera are *Nitrosomonas* and *Nitrobacter* for ammonia and nitrite oxidation, respectively. Nitrification is slower than denitrification, and if too much organic carbon (BOD) is present, nitrification processes will often be overshadowed by aerobic heterotrophic bacteria. In general, nitrification is favorable with high oxygen and ammonia concentrations and low BOD concentrations. As such, nitrification is often the primary nitrogen transformation process in VFTW, where high levels of aeration are easily achievable due to the incorporation of environmental oxygen between wastewater applications to the media.

Denitrification: Denitrification completes the nitrogen transformation for wastewater treatment, transforming nitrate into gaseous dinitrogen, which releases into

the atmosphere (Vymazal, 2007). The overall denitrification reaction can be simplified as follows:

$$3(CH_2O) + 2NO_3^- \rightarrow 3CO_2 + N_2 + 3H_2O$$

Key to this reaction are the presence of an organic carbon source and the absence of oxygen. Denitrification is mainly performed by heterotrophic denitrifying bacteria, such as the genera *Bacillus* and *Pseudomonas*, though a wide variety of bacteria are capable of denitrification (Lee et al., 2009). In an anaerobic or anoxic environment, denitrifying bacteria use oxidized nitrogen (usually NO_3^- formed from nitrification) as an electron acceptor and organic carbon as an electron donor. This process is complex, involving intermediate species before transformation to dinitrogen. The sequence is simplified as follows:

$$NO_3^- \rightarrow NO_2^- \rightarrow NO \rightarrow N_2O \rightarrow N_2$$

Denitrification is more difficult to achieve than nitrification in a VFTW due to the incorporation of air into the media (Dotro et al., 2017). This difficulty can be offset by increasing saturation of the media. While nitrification is enhanced by frequent, small dose volumes of wastewater to maximize oxygen content, large dose volumes can stifle oxygen and create a more favorable denitrification environment.

Both nitrification and denitrification are critical to effective nitrogen removal in wastewater. Nitrogen is most innocuous as dinitrogen gas, but this transformation requires the nitrogen to be present as nitrate, not ammonia. Because influent contains primarily ammonium, nitrification must occur before denitrification can occur. However, it is also beneficial to perform denitrification first to use most of the organic carbon

before undergoing nitrification, which is inhibited by excessive organic carbon. Nitrification benefits from higher pH but lowers the pH as it occurs, while denitrification raises the wastewater pH. Optimization of nitrogen removal and overall performance of a VFTW requires that neither process occur ideally, as both must be balanced and sequenced.

Physiochemical Nitrogen Transformation

Though generally not significant in a TW, ammonia volatilization, ammonium adsorption, and sedimentation are important processes to consider. Ammonia volatilization primarily occurs in primary treatment during wastewater ammonification. While most organic nitrogen transforms into ammonium, a fraction remains unprotonated as ammonia, which can then volatilize to a gaseous state and escape to the atmosphere (Vymazal, 2007). This fraction is generally insignificant for domestic wastewater with pH below 7.5, but can become significant should the pH increase toward the pK_a of 9.3. Ammonium adsorption is most significant during wetland startup, as ammonium readily adsorbs to the new media (Dotro et al., 2017). However, the media will quickly reach its sorption capacity, at which point additional ammonium adsorption will be nearly zero. This process may become notable again should the ammonium become desorbed from the media. In a VFTW, this commonly occurs during the rest period between applications of wastewater. Ammonium sorbs to the media during application, then desorbs and nitrifies when the saturation level sufficiently decreases (Morvannou et al., 2014). The extent to which this occurs depends on the frequency of media saturation.

Lastly, sedimentation is the primary process removing most remnant particulate organic nitrogen from the wastewater (Lee et al., 2009). Particulate nitrogen settles

through the media, adhering to plant roots to later be mineralized and used as nutrients. The resulting changes in dissolved nitrogen concentrations can be difficult to quantify but is likely insignificant compared to influent dissolved nitrogen concentrations treated by biological processes.

Hydraulic Loading Effects

The hydraulic loading rate (HLR) of a TW affects all processes of contaminant removal. HLR measures the volume of water applied to the surface area of the wetland, commonly presented as cm/d. Analysis of HLR effects is difficult, as TW systems will react differently to different hydraulic loads depending on media size and influent water quality. Still, it is important to consider hydraulic loading effects on nitrification and denitrification when attempting to optimize system design.

Standard kinetic models demonstrate that nitrification is most directly affected by ammonia concentration, but changes in hydraulic loading rate can also have consequences for nitrogen removal performance. Higher hydraulic loading delivers more ammonium to the TW over a given time, potentially increasing the quantity of ammonium nitrified without changes in concentration. The combined effect of concentration and flow rate can be estimated from an ammonium loading rate (presented as g/m^2d) but masks the independent effects of each parameter. In general, increased HLR and ammonium loading lead to improved nitrification despite reduced substrate contact time (Saeed and Sun, 2012).

Exploration of independent HLR effects is primarily based in theory. One potential negative effect of increased HLR is inhibition of ammonium adsorption to substrate, limiting nitrification (Molle et al., 2008). If water moves through the wetland

bed faster than bacteria can transform the ammonium, it is reasonable that some ammonium flows through untreated. Also, agitation from an increased flow rate could desorb ammonium previously fixed to substrate or the media, creating an unsteady state of ammonia adsorption and disrupting the normal biological processes. Another potential negative effect could occur if the hydraulic loading rate is high enough to oversaturate the wetland, preventing the aerobic zone from being sufficiently renewed between doses, or flooding it and creating a permanently anaerobic environment. Paing et al (2014) observed decreased performance and increased variability in the first stage of a two stage French system, with removal of organic nitrogen measured as total Kjeldahl nitrogen (TKN) decreasing from 93 ± 7% to 72 ± 24% when hydraulic loading rate exceeded 60 cm/d.

Most TW operate at HLR lower than 60 cm/d, but many VFTW systems share the finding that, at lower HLR, ammonia removal improves as HLR and ammonia mass loading increases (Kantawanichkul et al., 1999; Stefanakis and Tsihrintzis, 2012). These findings suggest that, for a given VFTW system, nitrification increases up to a maximum hydraulic loading rate but there is an upper limit at which performance declines.

Denitrification processes are affected by HLR similarly to nitrification, with performance improving to an upper limit, then declining. In this case, the effect is difficult to separate from nitrate and organic carbon loading, which are both considered to limit denitrification (Lin et al., 2008). Almeida (2017) found that nitrate removal in a VFTW improved with increasing HLR and nitrate mass loading until they reached 23.9 cm/d and 20.4 g/m^2d, respectively, after which performance declined. Compared to nitrification, it is expected that denitrification is less sensitive to higher HLR, as it is an

anoxic process and the risk of oversaturation is avoided. Little data exists for high HLR nitrate removal in a VFTW, particularly at low nitrate concentrations, and thus more testing must occur to fully separate the effects of HLR, mass loading, and organic carbon loading on denitrification.

Vertical Flow Treatment Wetland Performance

Most VFTW systems share the same major design tenets, but the effect of many controlling variables remain unquantified. For example, media size, wetland bed depth and surface area, recycle, and number of stages can affect system performance in addition to the variability of the environment and the influent wastewater conditions (Dotro et al., 2017). The size of the media and wetland bed primarily affect the system residence time in response to HLR, providing necessary pore space and substrate contact area for reactions. The number of stages, often with recycle, are more important parameters affecting overall contaminant removal. VFTW systems are designed to favor creation of an aerobic zone by intermittent dose loading and resting periods, but this zone can disappear as the media becomes more saturated.

If only organic carbon and ammonium removal are required, a single stage can be optimized for both aerobic organic carbon mineralization and nitrification, though two stages are often utilized to better sequence the processes. If total nitrogen removal is required from the system, it becomes advantageous to use a two-stage system with recycle. In this application, the first stage is designed for organic carbon removal and denitrification and the second for nitrification. Most organic carbon is removed by a combination aerobic and denitrification activities within the first stage with the nitrate generated in the second recycled back to fuel denitrification. This design is often referred

to as the Modified Ludzak-Ettinger Process (Liu and Wang, 2017). Any remaining organic carbon is removed in the second stage, but its primary function is nitrification. Removal mechanisms for organic carbon in the first stage must be carefully balanced. If too much is removed by aerobic processes, there may be an insufficient amount for denitrification, but if too little organic carbon is removed by denitrification the excess bleeding to the second stage can disrupt the nitrification process. This creates a negative feedback loop, and less available nitrate can inhibit total nitrogen removal. Balance of the two stages is achieved by controlling the rate of recycle and level of saturation of the first stage. Low recycle leads to poor nitrogen removal (discharge with high quantities of nitrate), but high recycle risks hydraulic overload of the system. A recycle rate of 100% to 200% relative into inflow is considered optimal (Arias et al., 2010). Other combinations of TW designs could provide better removals, such as inclusion of a HF stage or additional stages, but at a significant increase in system size. For example, a three-stage system utilizing an aerobic VF stage, an anaerobic VF stage, and a HF stage for municipal sewage achieved total nitrogen removal of 79.9% (Vymazal, 2015).

Despite design variability, VFTW systems are consistently effective at removal of TSS, COD, and ammonia with > 90% removal for each (Dotro et al., 2017). Overall nitrogen removal especially without recycle, however, is typically < 20%. This is consistent with the expectation that VFTW systems excel at nitrification and therefore ammonium transformation, but struggle to denitrify the resulting nitrate. This is echoed by Langergraber (2010), who compares removal efficiencies for a single-stage and two-stage VFTW without recycle. These results are summarized in Table 1.

Table 1. Single-stage and two-stage VFTW system performance for COD, ammonia, and total nitrogen removal from Langergraber (2010).

System Design	COD % Removal	NH_4^+-N % Removal	TN % Removal
Single-stage VFTW	96.4	99.9	12.9
Two-stage VFTW	95.9	99.9	48.5

In addition to confirming the effectiveness of VFTW for removal of COD and ammonia, these results show that a two-stage VFTW is far more effective at removing total nitrogen than a single-stage system, even without recycle. The second stage in series (functionally the denitrification stage) was significantly improved through use of coarser media and a drainage layer, leading to better nitrate removal (Langergraber et al., 2008). The additional improvement of recycle can be seen in results from the Bridger Bowl VFTW in 2016 and 2017, a similarly designed two-stage system but with recycle. These results are shown in Table 2 (Woodhouse, 2018).

Table 2. Bridger Bowl VFTW system performance for COD, ammonia, and total nitrogen removal in system years 2016 and 2017 (Woodhouse, 2018).

System Year	COD % Removal	NH_4^+-N % Removal	TN % Removal
2016	93.0	97.4	69.6
2017	94.9	98.0	74.8

Removal of COD and ammonia remain effective, and total nitrogen removal improved to the 70-75% range. Note that varied recycle rates were used and can be found in Woodhouse (2018). System design and operational parameters for the Bridger Bowl system led to improved denitrification performance while maintaining the expected COD and ammonia removal.

Conclusion

While many processes occur in VFTW systems, the biological processes of nitrification and denitrification are core to their design for effective removal of organic carbon and nitrogen. Mass loading of COD, ammonium, and nitrate dictate system performance, but hydraulic loading rate must also be considered, as an upper limit of the hydraulic load likely exists where effectiveness declines regardless of mass loading of the constituent to be removed. Under most circumstances, VFTW systems excel at removal of COD and ammonia, and by using a two-stage system design with recycle, denitrification performance can be improved for a well-rounded wastewater treatment system. While the complex, interconnected variables make optimization difficult, two-stage VFTW systems show room for improvement as a secondary wastewater treatment system.

METHODS

Optimization of operational parameters for the Bridger Bowl experimental vertical flow treatment wetland (VFTW) have been developed over several years by multiple researchers with different goals. This section reviews the general site history, physical and operational design of the treatment wetland, established laboratory methods, and a brief overview of data analysis and noteworthy statistics. Further information about site construction and preliminary setup can be found in Moss (2016), and exploration of operating parameters and establishment of most current practices can be found in Woodhouse (2018).

Site Background

The Bridger Bowl Ski Area, which hosts the experimental treatment wetland of study, is situated northeast of Bozeman, Montana, on the east slope of the Bridger Mountain Range. A popular destination just 30 km from the Montana State University campus, Bridger Bowl has reliable wastewater flows and the location allows for convenient maintenance and sampling. The treatment wetland is located under the Virginia City lift, on the border of the Coyote Flats ski run between the main lower lodges and the Deer Park Chalet. As of Summer 2018, it shares this space with the full-scale treatment wetland that was designed, in part, by utilizing data collected previously from the experimental VFTW system.

The treatment wetland processes waste from the lower lodges of the ski area, and as such is operated primarily during the ski season, typically from mid-December to early April. Bridger Bowl receives approximately 9 m of snow annually, and during the operating season air temperatures can drop as low as -17°C, as measured at the Alpine

Lodge during the 2018 – 2019 ski season. These extreme weather conditions, when considered alongside the high-strength wastewater, allow for this system to be a study of the efficacy of wastewater treatment wetlands in a high stress environment.

System Design

The pilot-scale experimental system is a two-stage vertical flow treatment wetland. Treatment begins within two A cells (A1 and A2) and progresses to two B cells (B1 and B2). The two cells of each stage are identical and operated in parallel with mixing of individual cell effluent between stages. All cells have square surface areas of 23.8 m^2, with a depth of approximately 1.2 m and 26 cm freeboard. The cells have layered media, beginning with a bottom drainage layer, followed by transition, treatment, and protective layers. Each cell is lined with a geotextile fabric to create a watertight environment and sits on a 5 cm sand layer for support. Distribution and collection pipes are located immediately below the protective layer and within the drainage layer, respectively.

The drainage layer has a depth of approximately 10 cm from the bottom liner and consists of mixed cobble and gravel ($d_{50} \approx$ 50-100 mm), allowing for flow of oxygen and wastewater to the bottom of the cell. The transition layer, also 10 cm thick, uses pea gravel ($d_{50} \approx$ 10 mm) to create a buffer zone preventing media from escaping the overlying treatment layer. The treatment layer consists of gravel ($d_{50} \approx$ 5 mm) in the A cells and sand ($d_{50} \approx$ 0.6 mm) in the B cells, with an approximate thickness of 62 cm for each. This layer supports most of the microbial activity treating the water. The A cell media is coarser to prevent buildup of carryover solids after primary wastewater treatment. Above this, the protective layer is approximately 10 cm thick and consists of

coarse gravel ($d_{50} \approx 5$ mm, same as the treatment layer of the A cells), protecting the operator and wetland from contamination and insulating the treatment layer from the winter cold and snow.

Before entering the treatment wetland, wastewater from the Jim Bridger and Saddle Peak base lodges undergoes pretreatment in a series of septic tanks at the base. These tanks had a capacity of 87 m^3 (23,000 gal) prior to the 2018 season, when capacity was increased to 169 m^3 (45,000 gal). This post-primary wastewater is then pumped to a 75 m^3 (20,000 gal) surge tank adjacent to the research and full-scale treatment wetlands. Water is transfer from this surge tank to a 3.8 m^3 tank which serves as a pump chamber to the experimental VFTW and has previously been referred to as the septic tank (Moss, 2016; Woodhouse, 2018), thus this nomenclature will be retained.

Within the experimental wetland system, water is dosed from the septic tank onto the A cells for treatment, and the effluent collected from both cells enters a 3.8 m^3 transfer tank. This combined A-cell effluent is then dosed onto the B cells, before entering a final 5.7 m^3 recirculation tank. The system has recycle capabilities, and a portion of this final effluent can be pumped directly back onto the A cells to improve treatment. A schematic of the system is shown in Figure 1 (Woodhouse, 2018).

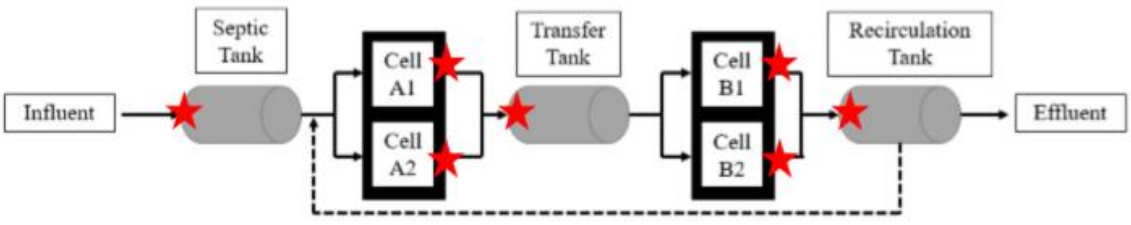

Figure 1. Bridger Bowl VFTW schematic, with stars representing sample locations.

Wastewater enters the cells through the distribution pipes, driven by mechanical pumps for even dispersal. A 2-inch PVC pipe bisects each cell and is perpendicularly branched by 1¼-inch pipe laterals at an interval of 50 cm. Each lateral has 8 mm orifices spaced at 33 cm. The entire distribution system is placed immediately over the treatment layer and hence within the protective layer. The collection pipes consist of standard 4-inch drainpipe set within the drainage layer, distributed in a pattern similar to the distribution pipes but at 107 cm intervals. The collection line of each cell is attached to an Agri-drain© Inline Water Level Control Structure™ to allow user control and monitoring of water level within the cell.

The wetland cells were planted with the macrophyte species *Carex utriculata* (beaked sedge) and *Schoenoplectus acutus* (hardstem bulrush) in 2013. Research at MSU has shown that, in addition to being robust and native, these species have superior removal of COD and TN compared to other studied wetland plants (Taylor et al., 2010; Allen et al., 2013). Originally planted with monocultures of each species in opposite quadrants of the cells, the distribution of the species has become more random over time. Despite weeding efforts, some unknown plant species now grow and compete for space with the *Carex* and *Schoenoplectus*, adding a degree of uncertainty to the treatment characteristics of the wetland plants. A tall fence surrounds each set of cells to protect them from skiers and wildlife. Additional details of the system construction and start-up periods can be found in Moss (2016).

Study Design

This study focuses on data collected during the 2017-2018 and 2018-2019 ski seasons, hereafter referred to as the 2018 and 2019 seasons to be consistent with earlier

studies. For 2018 and 2019, the system operated at the previously established optimal operational parameters. These parameters, namely the dosing frequency, recycle ratio, and saturation level, were evaluated by Woodhouse (2018), and are not changed through the course of this study. The dosing frequency is twelve per day, utilizing the following dosing schedule. Over a 2-hour period the A cells are dosed once with a predetermined volume of post-primary (septic) water from the septic tank followed by three doses of water recycled from the B cells. The B cells are dosed with the combined flow of septic and recycled water (transfer load) once in the 2-hour period. Timing is such that each dose has ample time to drain unsaturated layers before the next dose is applied. The recycle ratio is 2:1, with two volumes of recirculated water per volume of septic water applied to the A cells. The saturation levels of the A and B cells are 71 cm and 0 cm, respectively. Later schemes from Woodhouse (2018) that match these parameters are also presented in Table 3 for comparison with present data. Note that in 2017 the A1 and A2 cells were at different saturation levels, so only A2 data in which the saturation level was 71 cm is used for comparison. With these operating parameters established, this study can focus wholly on manipulation of the influent flow volume to achieve higher hydraulic loading rates.

Table 3. Operational parameters for schemes in system years 2017, 2018, and 2019. Schemes in 2017 from Woodhouse (2018).

System Year	Scheme Date	Scheme #	Septic Volume (gal/d)	Septic Hydraulic Load (cm/d)	Septic Dose Load (cm)	Recycle Dose Load (cm)	Transfer Hydraulic Load (cm/d)	Transfer Dose Load (cm)
2017	1/25 – 2/23	7	1295	10.3	0.86	0.65	33.6	2.80
	2/23 – 4/2	8	1701	13.5	1.13	0.82	43.2	3.60
2018	12/10 – 1/13	9	1999	15.9	1.33	0.93	47.8	3.98
	1/13 – 2/14	10	1698	13.5	1.13	0.77	40.6	3.38
2019	12/19 – 2/22	11	1501	11.9	1.00	0.69	35.8	2.98
	2/27 – 3/9	12	1999	15.9	1.33	0.93	47.8	3.98
	3/13 – 4/7	13	2422	19.3	1.61	1.06	59.7	4.98

All flow rates were calculated using empirical calibration curves with pump run time as the input. The daily volume of influent septic wastewater is a key point of control for the system. Recycle dose load and transfer dose load are also operational parameters set by the timing and duration of pump operation. Septic hydraulic load, recycle dose load, and transfer hydraulic load represent these inputs accounting for time and surface area. As the transfer hydraulic load represents the total daily volume of water moving through the system (the only variable distinguishing a scheme in this study), it will be used to distinguish schemes hereon.

Water samples were taken using two different methods. Composite samples were taken automatically by a programmable autosampler. The autosampler has capacity for 40 different 500 mL Nalgene sample bottles, each of which receives water pumped directly from one of seven sampling locations throughout the wetland system. The sampling locations are the septic, transfer, and recycle tanks and effluent from the four cells; A1, A2, B1, and B2. On a specified sample day, the composite sample is comprised of two volumes (approximately 250 mL each) taken approximately 12 hours apart. Sampling frequency was typically every other operational day. Grab samples were taken directly from their respective tanks using a long metal rod fastened with a 500 mL polyethylene bottle. A1 and A2 were sampled from weirs in the transfer tank, and B1 and B2 were sampled from weirs in the recirculation tank.

All water samples were preserved using 10 mL of 1.8 M sulfuric acid, either in the sample bottle before placement on the autosampler or immediately after taken as a grab sample, lowering the pH to below 2. Grab sample duplicates were taken and left unpreserved to periodically check the effects of acidification. The samples were placed in

snow for storage and additional preservation before being transported back to the lab. These procedures are in line with EPA wastewater preservation suggestions, as acidification and chilling to 4°C allow the sample to be analyzed within 28 days for water quality (USEPA, 1982).

Both the pump system and the autosampler are controlled using a Supervisory Control and Data Acquisition (SCADA) system installed on a computer within an operations building adjacent to the cells, which also houses the autosampler. The system allows for operator input of a pump schedule in the format of a spreadsheet, including the timing and duration of a pump event. The system then loops this schedule for the specified timeframe to automate controls. It also allows for manual manipulation of each pump and valve, monitors pump activity, and has the capability to be programmed for a variety of situations.

Lab Methods

All water quality testing was conducted at the Environmental Engineering Lab at Montana State University. All samples were tested for nitrate, ammonium, and chemical oxygen demand (COD). Results for total nitrogen (TN) are the sum of nitrate and ammonium measurements. Periodically, selected samples were also tested for total Kjeldhal nitrogen (TKN).

Nitrate data was acquired according to Standard Methods 4110 using ion chromatography (IC). Analysis was conducted on a Metrohm IC with a Dionex AS22 fast column. This IC was used for nitrite data as well, but values were consistently below measurement range, so nitrite concentrations were deemed negligible. Periodically, samples were tested without prior acidification, so it is unlikely that the absence of nitrite

was caused by sample preservation practices. Ammonium data was acquired under Standard Methods 4500, using the Berthelot reaction in a colorimetric assay. TKN data was acquired using Hach Method 10242, which uses a peroxodisulfate digestion to compare nitrate and nitrite values with an undigested sample, with the resulting difference giving TKN. COD was measured using Standard Method 5220D (Hach Method 8000), which involves sample digestion and oxidation of organic matter by potassium dichromate. The TKN and COD tests were conducted from Hach kits containing all necessary reagents and vessels; these are the Simplified TKN (TNT880), Low Range (LR) COD (catalog number 2125815), and High Range (HR) COD (catalog number 2125915), respectively.

Data Analysis

Detection Limits

The detection limits for each test used and the number of samples falling below the detective limit are shown in Table 4. Note that any sample below range using High Range COD was retested and within range for Low Range COD, resulting in zero samples below range for COD. The number of nitrate and ammonium samples with values below the detection limit for a given year ranges from 12% to 48%, with only nitrate in system year 2019 being greater than 26%.

Table 4. Detection limits and number of samples below detection limit for system years 2018 and 2019

Test	NO_3	NH_4	LR COD	HR COD
Detection Limit (DL)	2.5 mg/L	1 mg/L	3 mg/L	20 mg/L
# Samples below DL (2018)	21 (12%)	42 (26%)	0	N/A
# Samples below DL (2019)	84 (48%)	36 (21%)	0	N/A

A method used previously to correct values below the detection limit for this system used the following equation (Croghan & Egeghy, 2003):

$$Corrected\ Value = Detection\ Limit/\sqrt{2}$$

This equation is intended for use when the number of samples below the detection limit is approximately 25%. In 2019, the A cells had consistently lower nitrate values, resulting in many measurements below range for influent septic and effluent from cells A1 and A2, whereas in 2018 only septic measurements were below range. Knowing this, and to be consistent with 2018 results, the above correction will be used for 2019 nitrate as well.

Statistical Analysis

All statistical analyses and figure preparation were completed using Matlab version R2019b. Relevant functions were used for linear regression and multivariate linear regression when appropriate. The significance level for results is 95% unless otherwise noted.

RESULTS & DISCUSSION

Water Quality

Improvement of water quality as it passes through a vertical flow treatment wetland (VFTW) is influenced by a host of potential inputs and operational parameters. The focus of this study is on the hydraulic loading rate (HLR), however concentrations and mass loading rates for each component of interest must also be considered. These parameters are not independent; increasing the hydraulic loading rate will necessarily increase mass loading rates, but should have minimal influence on concentrations. To assess possible interactions between parameters, results will first be presented as seasonal mean concentrations and removals, then as time series of concentrations, and finally as mass loading compared with mass removal. Results will be reported separately for 2018 and 2019, followed by combined 2018 and 2019 results. Finally, these will be considered alongside 2017 results when appropriate.

Performance Summary

To judge the system overall effectiveness for secondary wastewater treatment, the influent and effluent values for concentrations of COD, TN, NH_4^+, and NO_3^- are compared for system years 2018 and 2019 in Table 5. These were sampled from the septic and recirculation tanks for influent and effluent, respectively. Despite variable hydraulic flow conditions, results are presented as seasonal means, and therefore cannot be used to compare operating schemes. Of initial note in these results is the lower influent COD and TN concentrations compared to historical values for this system. Mean COD in the influent was 555 mg/L in 2018 and 607 mg/L in 2019, whereas 2016 and 2017 values were 900 mg/L and 969 mg/L, respectively (Woodhouse, 2018). Similarly, mean TN in

the influent was 141 mg/L in 2018 and 105 mg/L in 2019, but 2016 and 2017 values were 188 mg/L and 205 mg/L, respectively. These changes could be due to factors such as the increased volume of the new primary treatment tanks installed between the 2017 and 2018 seasons or unknown operational changes at the resort. This lower strength influent wastewater offers a unique opportunity to at least partially separate the influence of hydraulic load and mass constituent load on the system, as concentration is not a user-controlled parameter.

Table 5. Overall water quality of the VFTW in 2018 and 2019. The influent (septic tank) and effluent (recirculation tank) concentrations are mean values and SE is standard error for *n* samples tested.

2018							
Parameter	Influent	SE	*n*	Effluent	SE	*n*	% Removal
COD (mg/L)	555	28	23	25	1.8	23	95.4
TN (mg/L)	141	9.3	23	46	4.0	24	67.2
NH_4^+-N (mg/L	139	9.3	23	0.7*	0.2	21	99.5
NO_3^-N (mg/L)	1.7*	0.1	24	46	4.1	24	N/A
2019							
Parameter	Influent	SE	*n*	Effluent	SE	*n*	% Removal
COD (mg/L)	607	17	25	25	2.6	25	95.9
TN (mg/L)	105	4.4	25	48	3.9	25	54.1
NH_4^+-N (mg/L	105	4.4	25	4.2	1.3	25	96.0
NO_3^-N (mg/L)	1.7*	0.01	25	44	3.0	25	N/A

*Under range, result from DL correction

Consistent with prior results, the system effectively removed most COD and ammonium (> 95%), indicating effective nitrification in the system. Overall TN removal was sufficient at 67% for 2018 and 54% for 2019, though this shows room for improvement in future operation. Woodhouse (2018) also considered removals of TSS, BOD_5, and phosphate (PO_4^{3-}) for the system, but sample sizes were small (n < 13) due to the need for additional testing kits for phosphate and extended testing time for TSS and BOD_5. TSS removal was 98% in 2017 and is not expected to vary seasonally. BOD_5 is an important measure of organic carbon, but can be approximated by COD, which is more

easily tested. Additionally, changes in COD in the system are primarily due to biological processes, and are thus representative of changes to BOD_5. Phosphorous removal is necessary in secondary wastewater treatment, and is monitored monthly in the final effluent, but it is not a design parameter for the VFTW. Though not tested in the current study, removal of PO_4-P in 2018 and 2019 would be expected to be similar to 2017 values (34%).

Time Series Results

Variation within each season of the measured COD, ammonium and nitrate concentrations in the septic, transfer, and recirculation tanks are presented in Figures 2-4, respectively. The vertical lines represent the dates of schemes changes on January 13, 2018, February 27, 2019, and March 13, 2019 (see Table 3).

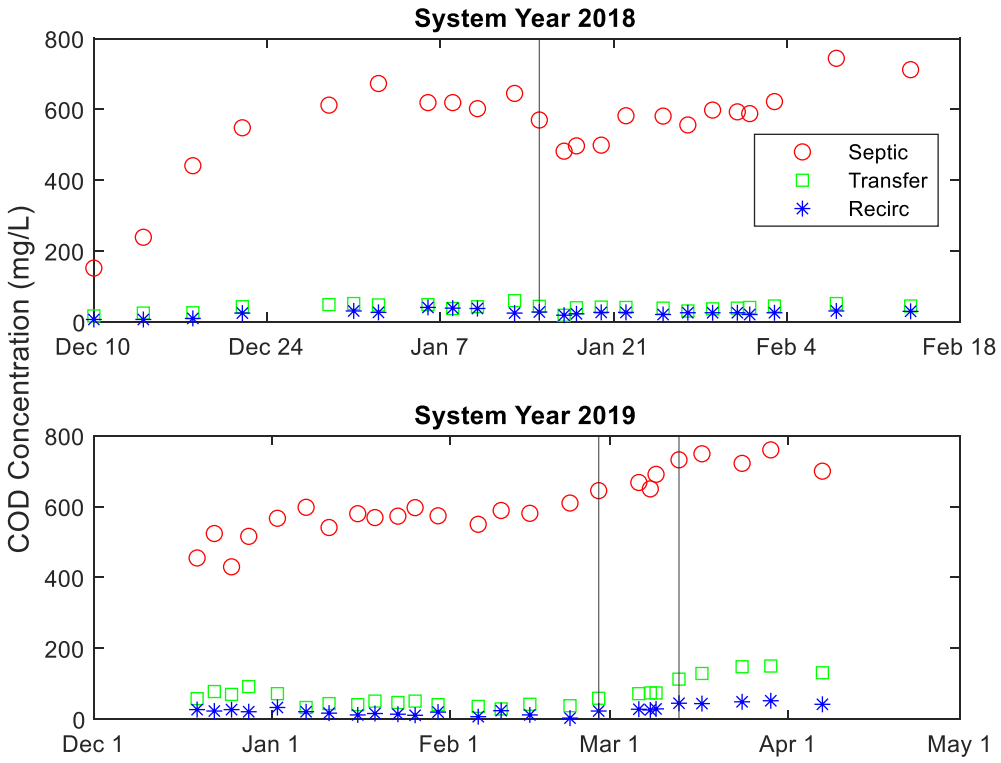

Figure 2. Time series of measured COD concentration in the septic, transfer, and recirculation tanks for system years 2018 and 2019. Vertical lines represent changes in the hydraulic loading rate (Schemes 9-13).

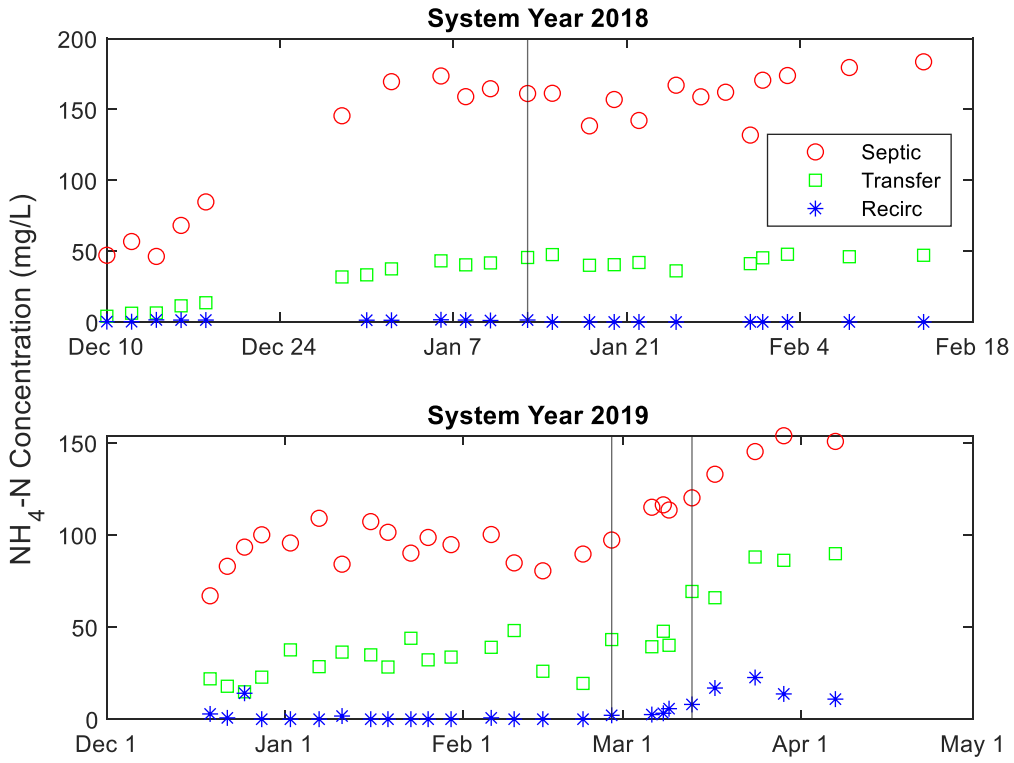

Figure 3. Time series of measured ammonium concentration in the septic, transfer, and recirculation tanks for system years 2018 and 2019. Vertical lines represent changes in the hydraulic loading rate (Schemes 9-13).

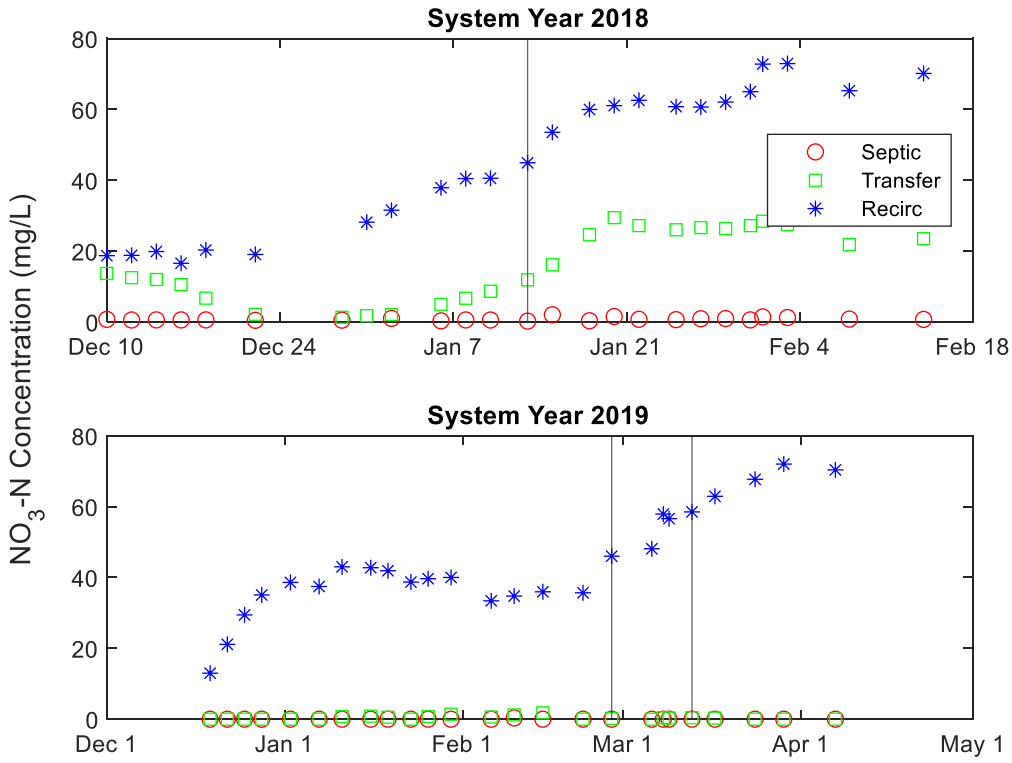

Figure 4. Time series of measured nitrate concentration in the septic, transfer, and recirculation tanks for system years 2018 and 2019. Vertical lines represent changes in the hydraulic loading rate (Schemes 9-13).

In both seasons, septic COD concentration, representing the strength of the influent wastewater, increases steadily from the beginning of the season, but with some variation due to variation in the number of skier visits (Fig. 2). COD removal occurs primarily in the A cells, shown by the large drop in concentration from the septic to transfer tanks. Virtually all remaining COD is then removed in the B cells. Transfer tank COD concentrations are consistently low (<92 mg/L) until the shift from Scheme 12 to Scheme 13 in system year 2019, corresponding to an increase in the transfer HLR from

47.8 to 59.7 cm/d, when COD increases to a peak of 150 mg/L on March 29. This indicates that COD removal in the A cells declined at the highest flow rate.

As with COD concentrations, septic tank ammonium concentrations increase from the beginning of the season as wastewater strength increases and varies with visitor numbers (Fig. 3). While some nitrification likely occurs in the A cells, the decrease in concentration between the septic and transfer tanks is mostly due to dilution from the system recycle. Because all schemes used a 2:1 recycle ratio and there was very little ammonium in the recycle tank, the transfer tank ammonium concentration should be approximately one-third of the septic concentration from dilution alone. Nitrification primarily occurs in the B cells, shown by the decrease in ammonium concentration from the transfer tank to the recirculation tank. This B cell nitrification consistently removed almost all ammonium from the wastewater, although some ammonium remained at the highest influent flow in system year 2019, again indicating a decrease in system effectiveness at this highest flow rate.

Influent nitrogen is arguably better represented by total Kjeldhal nitrogen (TKN) as it measures organic nitrogen as well as ammonia, however in most situations TKN and ammonium concentrations are often similar due to the rapid conversion of organic nitrogen to ammonium. Due to cost, TKN measurements were taken only on a limited basis. The effectiveness of ammonium as an accurate representation of TKN was determined by analyzing the ratio of TKN to ammonium for all samples from the septic and transfer tanks for which both TKN and ammonium were available (Figure 5).

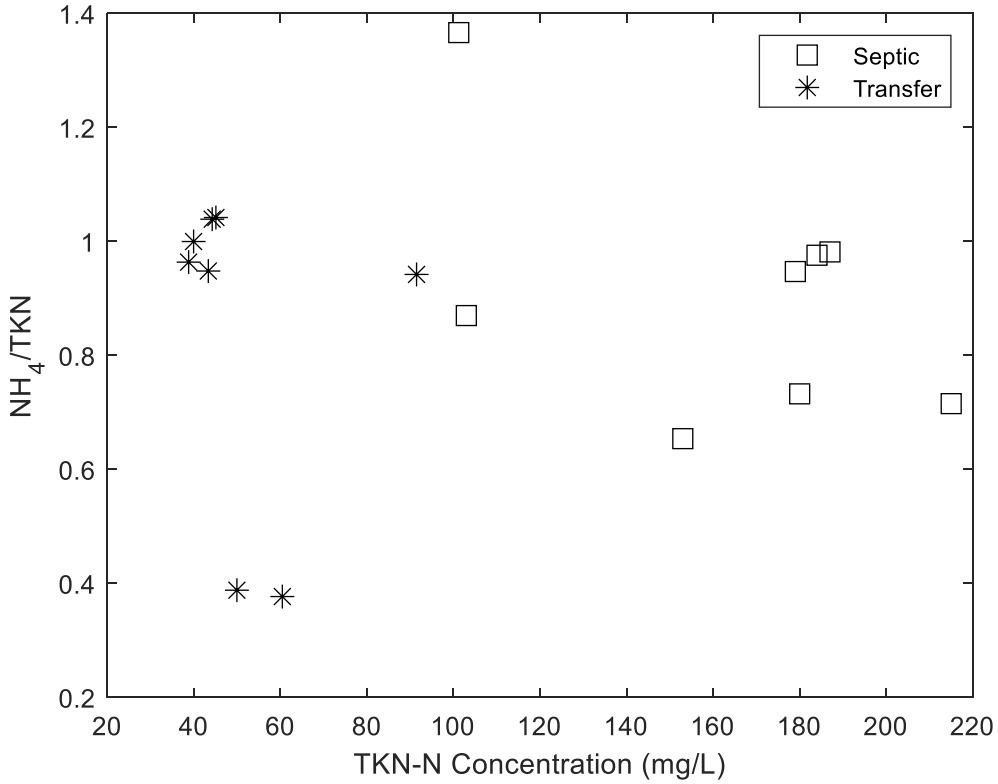

Figure 5. Measured ratio of NH_4^+ to TKN against measured TKN concentration in the septic and transfer tanks.

As expected, concentrations of both TKN and NH_4^+-N are higher in the septic tank than transfer tank but there is no obvious trend in the ratio with sample location or nitrogen concentration. The mean ratios of ammonium to TKN are 0.91±0.08 and 0.84±0.10 for the septic and transfer tanks, respectively. Any difference due to location should be reversed because ammonification should have continued during the time water travelled through the A cells. In addition, data scatter is large; some values are greater than one, a theoretically impossible situation. Based on these observations it is reasonable to consider ammonium concentrations an appropriate approximation of TKN hereafter.

Nitrate is present in the system almost exclusively as a product of internal nitrification, as shown by septic tank concentrations below the detection limit at all influent flow rates (Fig. 4). This nitrate, created primarily in the B cells, is then applied to the A cells via recycle, where it is removed by denitrification in conjunction with removal of biodegradable COD. This process was generally effective, as shown in system year 2019 when transfer tank nitrate concentrations were always near the detection limit, indicating nearly 100% nitrate removal in the A cells.

Due to the nearly complete nitrification in the B cells, changes in the recirculation tank nitrate concentration closely parallel changes in transfer tank ammonium concentration in most schemes (compare Figs. 2 and 3). However, in approximately mid-January of the 2018 season, generally good initial nitrate removal in the A cells appears to dramatically decrease, resulting in transfer tank nitrate concentrations around 20 mg/L (Figure 3). The increase roughly coincides with the shift from Scheme 9 to Scheme 10 but appears to start prior to this shift and is therefore likely not related to it. Reasons for the poorer performance are not clear, but the effect seems to be an anomaly because performance was consistently good in 2019. It is possible that the A cells became carbon limited, which would inhibit nitrate removal.

A and B Cells as Replicates

The pair of A cells and the pair of B cells are physically identical and during the term of this study were run under the same conditions using the same influent. This potentially allows for consolidation of data, increasing sample sizes for better statistical reliability. Table 6 displays results from paired t-tests for differences in concentrations of the main parameters between replicate A cells and replicate B cells for system years 2018

and 2019. The pairs are results from the A1 and A2 or B1 and B2 sample locations for a given sample day. Note that B cell ammonium is not included, as these ammonium measurements were consistently below the detection limit and thus would not be useful for this purpose. At the 5% significance level, only nitrate from the B cells showed a significant difference, with a p-value of 0.0033.

Table 6. A and B Cell paired t-test results for a mean difference of zero at a 5% significance level.

Measurement	A Cell COD	A Cell NO_3	A Cell NH_4	B Cell COD	B Cell NO_3
p-value	0.5885	0.1216	0.4421	0.4924	0.0033
n (pairs)	55	56	53	56	57

To further verify the B cell status as replicates, Figure 6 displays cell B2 nitrate measurements plotted against cell B1 nitrate measurements. Despite failing a test of similarity using the paired t-test, nitrate measurements from the B cells appear to be well correlated over the range of observed values, with only two data points showing greater than 10% variation between cells. Considering this is the only parameter showing a statistical difference between these potential replicates and that the difference is not practically relevant, the A1 and A2 cells and B1 and B2 cells are considered replicates of each other. Hereafter, A1 and A2 data will be combined as A cells, and B1 and B2 will be combined as B cells.

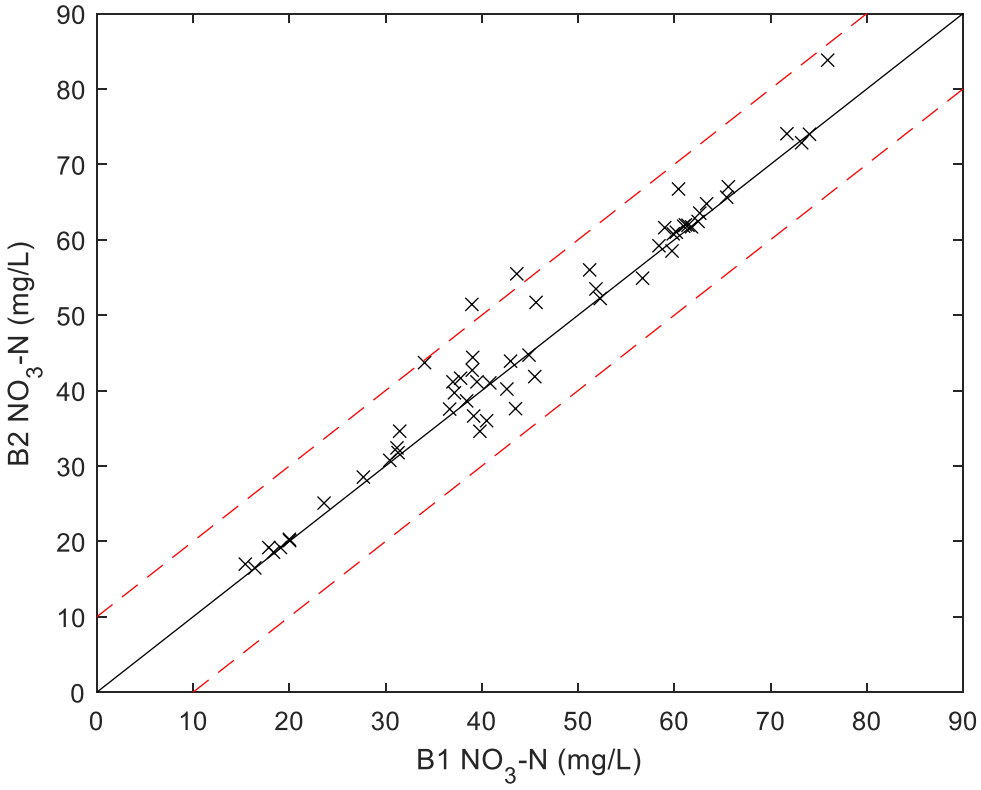

Figure 6. Visual comparison of B1 and B2 nitrate measurements against a line representing a 1:1 ratio. The red dashed lines represent 10% departures from a 1:1 ratio.

System Performance

The two key functions of the VFTW are to remove biodegradable organic COD and nitrify ammonium in the influent wastewater. The primary purpose of the A cells is to remove nearly all the COD to minimize COD interference on the B cell's ability transform influent ammonium to nitrate. However, by utilizing partial saturation and recycle, a significant proportion of COD can be removed by the denitrification process in the A cells thereby simultaneously achieving a second goal, improving system performance for total nitrogen removal by removing recycled nitrate. A delicate balance in operation of the A cells is required to achieve total nitrogen removal, some COD

should be removed by aerobic heterotrophic processes in the upper unsaturated layers to achieve an optimal COD-nitrate ratio in the lower saturated zone. Too much aerobic removal limits the denitrification potential of the A cells by providing too little organic carbon. Too little aerobic activity runs the risk of COD carryover to the B cells, limiting their nitrification potential and producing a negative feedback loop by providing too little nitrate to the saturated zone of the A cells, potentially further limiting the denitrification process and exacerbating B cell COD carryover. Thus, the three major transformation processes influencing system performance are intricately tied; underperformance of one will influence performance of the other two. Previous results obtained by Woodhouse (2018) determined that 2:1 recycle with a 71 cm saturated zone in the A cells was better than other tested conditions in achieving this balance, hence these conditions were used throughout this study. However other factors such as changes in the hydraulic loading rate and/or influent septic concentrations also likely influence this balance.

To assess the system effectiveness regarding total nitrogen removal, it is important to look holistically at nitrogen transformations in both the A and B cells. While some nitrification in the aerobic upper layer of the A cells likely occurs, it is not their primary purpose, and a significant proportion that might be nitrified would likely be denitrified in the lower saturated layer. Thus, any possible nitrification within the A cells cannot be measured directly, but can be estimated using stoichiometry and considering dilution. However, any estimation of denitrification within the lower saturated layer of the A cells is complicated by this potential unmeasured nitrate input. In addition, the quantity of organic carbon available for denitrification in the saturated zone of the A cells is unknown due to the unknown fraction of COD removed in the upper aerobic layer.

Nevertheless, net denitrification can be assessed by a mass balance of ammonium plus nitrate. Similarly, there may be some denitrification within the B cells, but the unsaturated conditions coupled with little input of nitrate or organic carbon would greatly favor nitrification of ammonium being the predominant process. Thus, nitrification in the B cells can be directly assessed by a mass balance of either ammonium reduction or nitrate production.

To assess overall system performance, removal of COD, ammonium and nitrate is compared to the mass loadings of each, first in the A cells, then in the B cells. Nitrification and denitrification processes can be inferred from this analysis subject to the limitations above.

COD Removal in the A Cells

Note that any reference to mass loading on the A cells represents loading from both the septic tank and recycle water. Additionally, a fraction of the applied COD is not biodegradable, thus cannot be removed. Using the analysis of Woodhouse (2018) the non-biodegradable fraction of influent COD is 28 mg/L in 2018 and 30 mg/L in 2019, near the mean measured COD concentrations in the final effluent (25 mg/L both years). Finally as described above, the analysis considers the sum of effects from aerobic heterotrophic activity and denitrification.

The mass removal of COD is plotted against mass load of COD to the A cells for system year 2018 in Figure 7. The mass load of COD to the A cells in 2018 ranged from 70 g/m^2d to 129 g/m^2d. A regression coefficient of 0.88 suggests that approximately 88% of applied COD is removed in the A cells with little distinction between the two hydraulic loading rates (HLR). The offset between the regression line and the 100%

removal line is due primarily to the non-biodegradable COD fraction loaded to the cells but not removed. This fraction could also be shown by the presence of a positive x-intercept. Assuming the non-biodegradable COD concentration is approximately 25-30 mg/L, the x-intercept should range between 10 and 15 g/m^{2}d compared to 8.3 g/m^{2}d predicted from the regression equation.

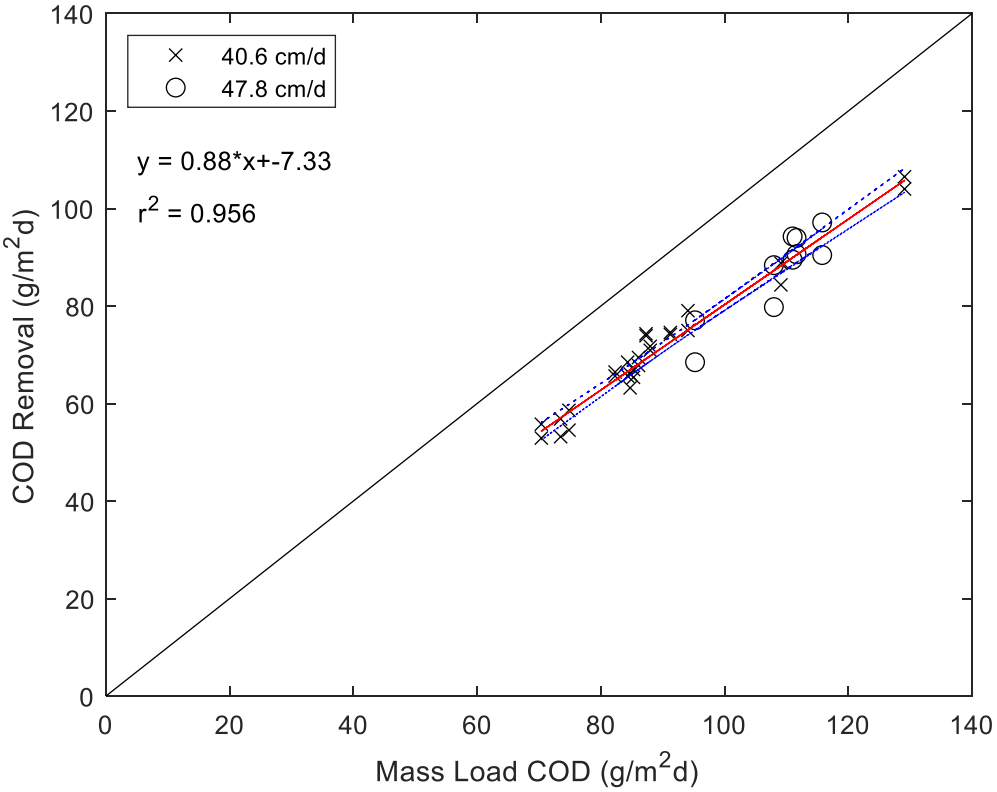

Figure 7. Mass removal of COD as a function of mass load of COD for the A cells in system year 2018, separated by total hydraulic loading rate. The 100% removal line is on the diagonal and a 95% confidence interval is the dotted line.

The mass removal of COD in the A cells is plotted similarly for system year 2019 in Figure 8. The mass load of COD to the A cells in 2019 ranged from 58 g/m^{2}d to 172 g/m^{2}d. A regression coefficient of 0.46 suggests that just 46% of applied COD is

removed in the A cells, but these data appear to be far less linear (r^2 = 0.69), with clear grouping based on hydraulic loading rate. Low removal rates for some data at the lowest HLR correspond to an apparent startup effect in the system; data from the first several sample events have the lowest septic tank concentrations and slightly elevated transfer tank COD concentrations (Figure 2).

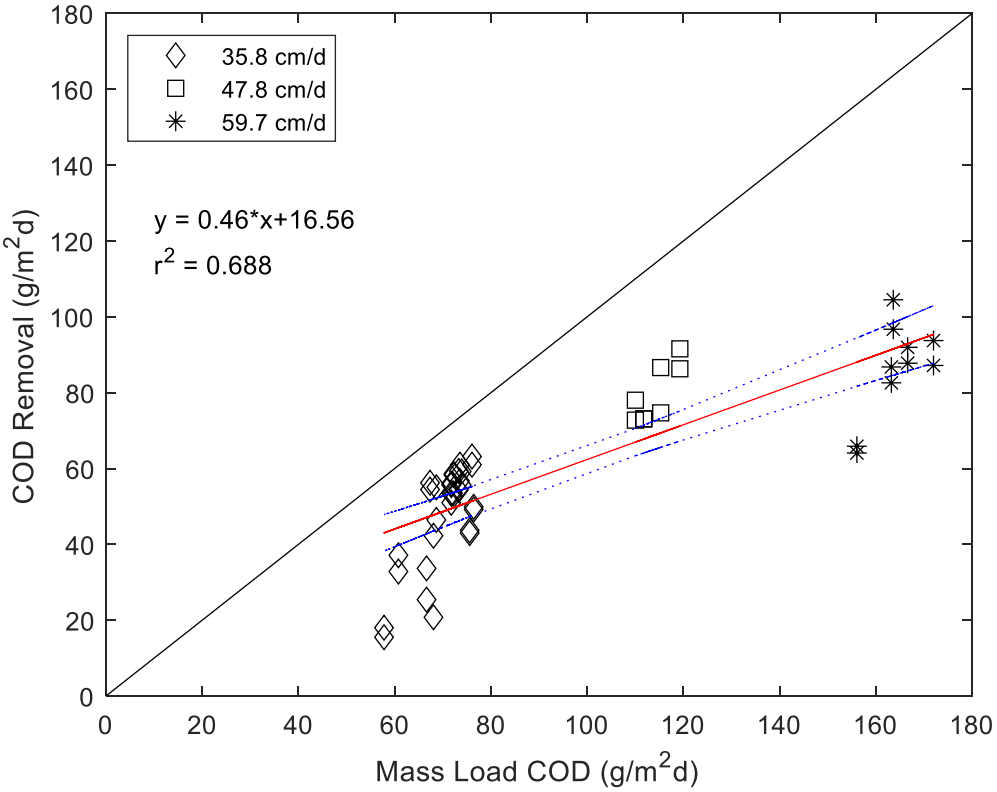

Figure 8. Mass removal of COD as a function of mass load of COD for the A cells in system year 2019, separated by total hydraulic loading rate. The 100% removal line is on the diagonal and a 95% confidence interval is the dotted line.

Over the entire range of mass COD loading the data display a downward curvature, which is made further apparent when plotted with 2018 data in Figure 9.With both years plotted together, it appears that COD removal is approximately linear for mass

COD loading of approximately 60 to 130 g/m^{2}d corresponding to total hydraulic loading rate between 35.8 cm/d and 47.8 cm/d, but at higher COD loading, especially at the 59.7 cm/d HLR removal does not increase despite higher loading. This is likely due to one or both of two confounding factors for effective COD removal; either the total HLR has reached its upper limit, or the COD mass loading rate has reached its upper limit.

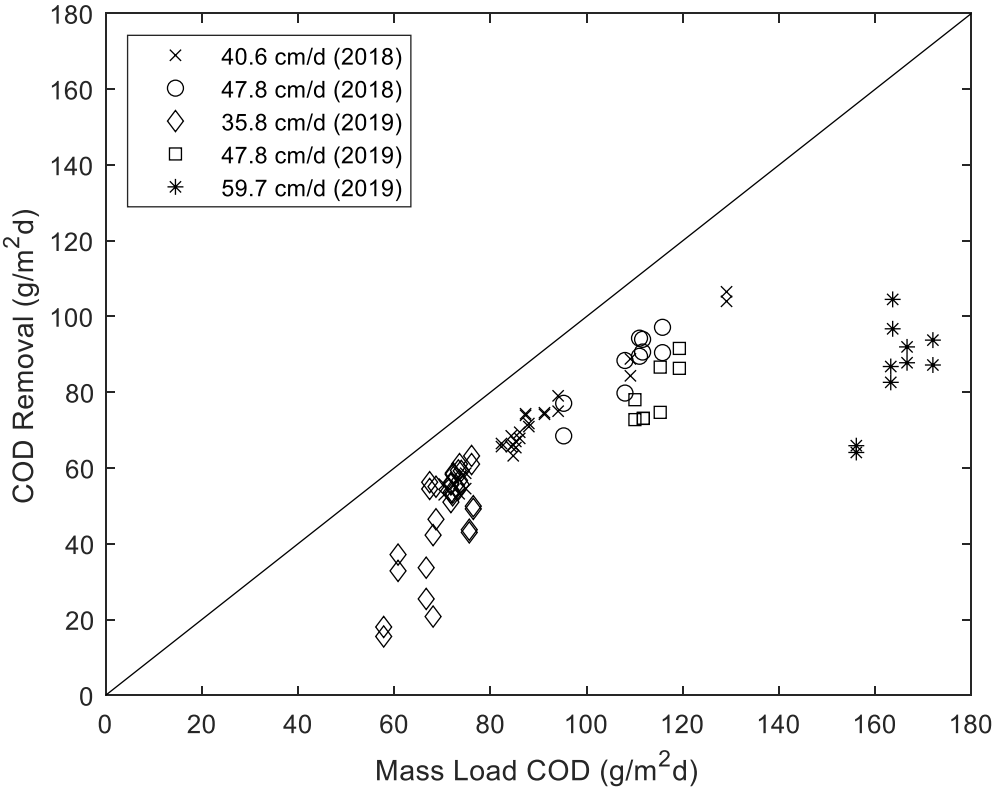

Figure 9. Mass removal of COD as a function of mass load of COD for the A cells for both system years 2018 and 2019, separated by total hydraulic loading rate. The 100% removal line is on the diagonal.

The relationship between mass loading and HLR can be further explored using a linear regression of 2019 data excluding the data at the total HLR of 59.7 cm/d, shown in Figure 10. With the highest flow rate excluded, the regression coefficient increases to

0.81, far closer to the 2018 value of 0.88, and the r^2 increases to 0.70 despite the smaller sample size. This observation forms the basis of exploration of the system hereafter, as an attempt is made to separate the confounding upper limits of constituent mass loading and hydraulic loading to maintain effective removal of organics and nitrogen in the A and B cells.

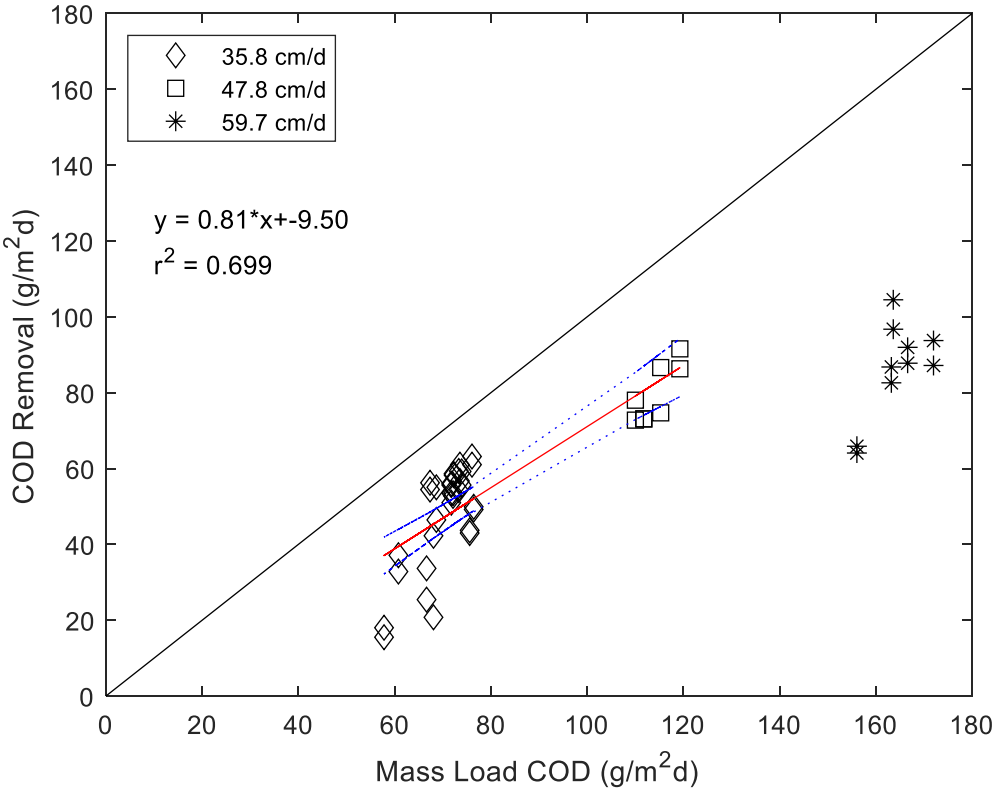

Figure 10. Mass removal of COD as a function of mass load of COD for the A cells in system year 2019, separated by total hydraulic loading rate. The 100% removal line is on the diagonal and a 95% confidence interval is the dotted line. The linear regression excludes data at the 59.7 cm/d hydraulic loading rate.

Combining data from 2018 and 2019 with the previously collected data from 2017 (Woodhouse, 2018) allows for some separation of the effects COD loading and HLR because the 2017 data represents influent of considerably higher COD concentration such

that mass loadings of COD are higher for the same hydraulic loading rate. The combined data are shown in Figure 11.

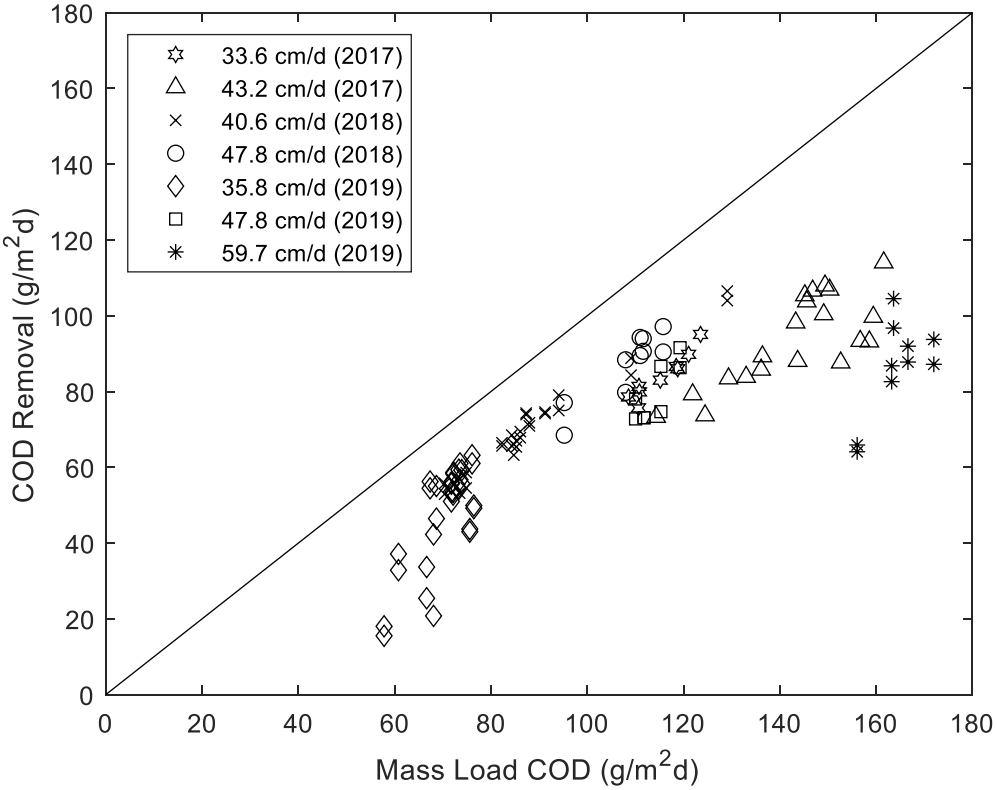

Figure 11. Mass removal of COD as a function of mass load of COD for the A cells for system years 2017 through 2019, separated by total hydraulic loading rate. The 100% removal line is on the diagonal. Data for 33.6 cm/d and 43.2 cm/d (2017) from Woodhouse (2018).

In 2017, COD loading onto the A cells at a hydraulic loading rate of 43.2 cm/d ranged from 114.3 g/m^{2}d to 161.6 g/m^{2}d. This slightly overlaps the 2019 COD loading at the 59.7 cm/d hydraulic loading rate, which ranged from 156.1 g/m^{2}d to 172.0 g/m^{2}d. Within the shared range of COD loading, average COD removal was 16% higher at the lower hydraulic loading rate in 2017, suggesting that the decreased removal performance

is due, at least in part, to the higher hydraulic loading rate in 2019. However, looking at the data set as a whole, when COD loading rates are greater than about 120 g/m^{2}d COD removal appears to decrease from a relatively consistent linear trend, suggesting this might be an upper limit to COD loading regardless of HLR. It is important to note that the above conclusions are valid only for the 71 cm saturation level (saturation levels are measured from the bottom liner of the cell); the 2017 data at a saturation level of only 53 cm indicates a consistent linear removal trend up to 160 g/m^{2}d (Woodhouse, 2018), thus saturation level influences the maximum allowable COD or hydraulic loading. Presumably this is because more aerobic respiration is possible at lower saturation levels. . Seasonal influences might also play a role, but the 2017 data at the 33.2 cm/d hydraulic loading rate fits well within 2018 and 2019 data, suggesting that observed differences are due to a combination of HLR and COD mass loading.

Ammonium Mass Removal in the A Cells

Mass removal of ammonium is plotted against total mass load of ammonium to the A cells for system year 2018 in Figure 12. As was the case with COD loading, any reference to mass loading on the A cells represents loading from both the septic tank and recycle water.

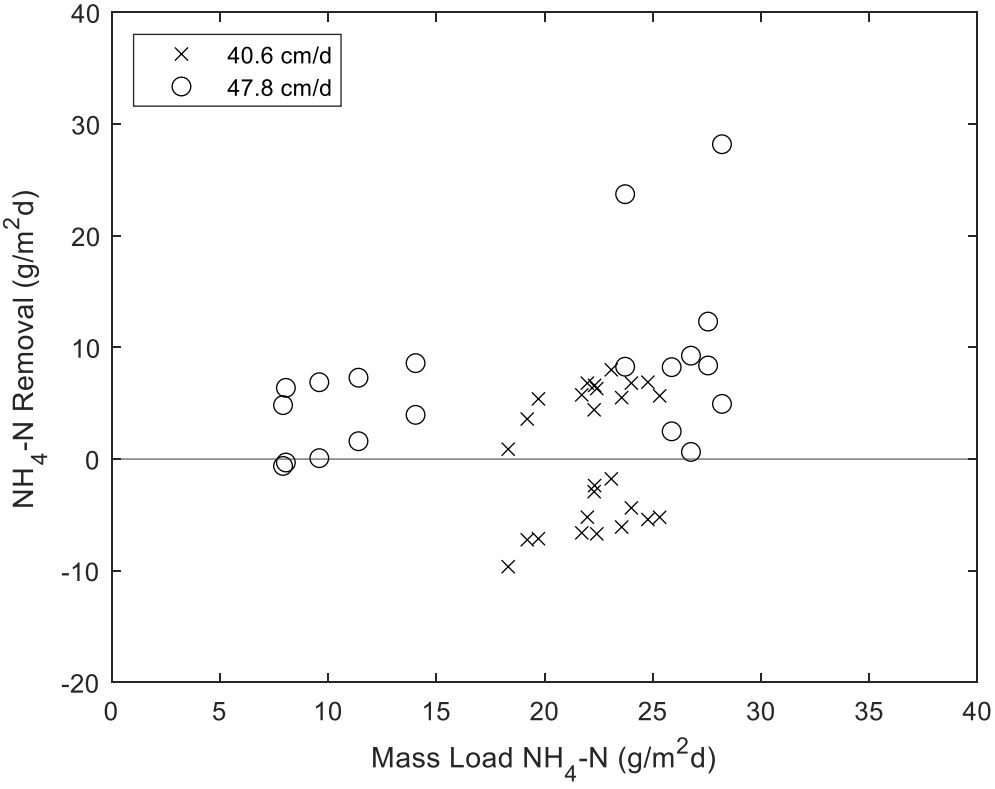

Figure 12. Mass removal of ammonium as a function of mass load of ammonium for the A cells in system year 2018, separated by total hydraulic loading rate.

In 2018, ammonium loading to the A cells ranged from 7.9 g/m^{2}d to 38 g/m^{2}d. A slight positive correlation between loading and removal of ammonium (especially within a specific HLR) indicates that a small amount of nitrification might be occurring in the A cells. However, the removal is often negative, suggesting ammonium formation or release. While large data scatter coupled with low removal surely influences this observation, it is possible that untargeted microbial processes result in ammonium generation. In addition, some applied ammonium is likely retarded relative to the hydraulic flow within the system due to sorption and desorption to the A cell media. This

time delay might be a partial component of the scatter because the calculated mass removed may not directly correlate with the calculated mass load.

The mass removal of ammonium in the A cells is plotted similarly for system year 2019 in Figure 13. In 2019, ammonium loading to the A cells was almost identical to the previous year, ranging from 8.7 g/m^{2}d to 38 g/m^{2}d. Despite large data scatter within a specific HLR, there is a clear trend toward ammonium production as ammonium and hydraulic loading rates increase. At the 59.7 cm/d hydraulic loading rate (corresponding to 27 g/m^{2}d to 38 g/m^{2}d mass loading), there is no removal and production ranges from 8.7 g/m^{2}d to 19 g/m^{2}d.

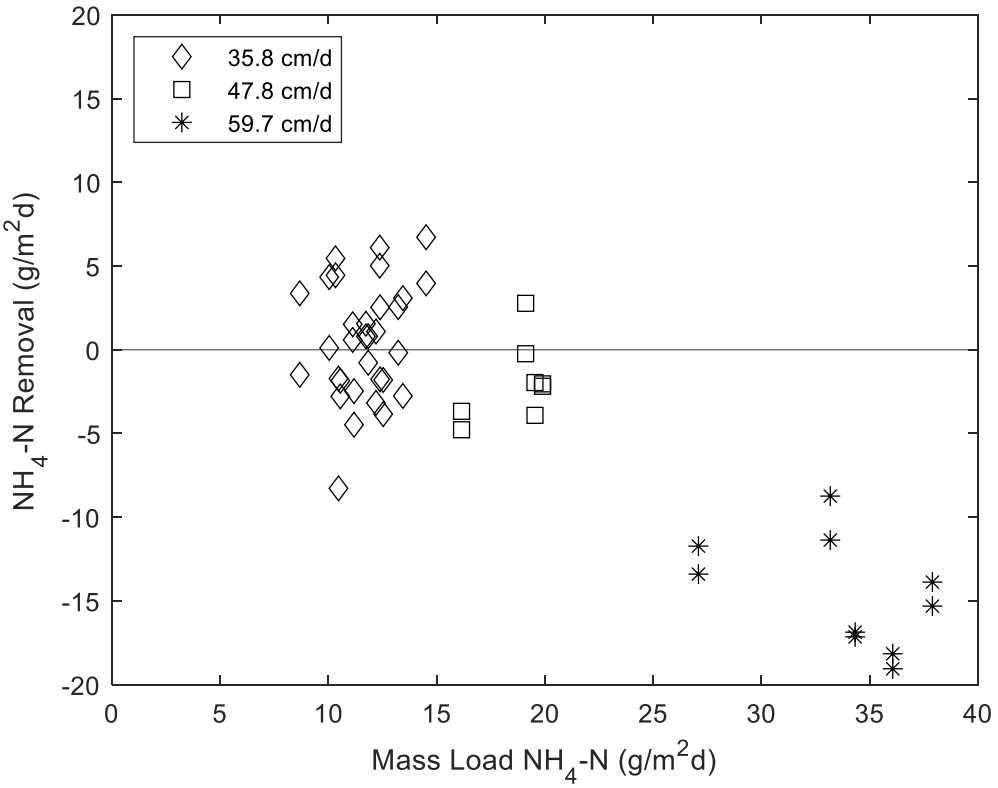

Figure 13. Mass removal of ammonium as a function of mass load of ammonium for the A cells in system year 2019, separated by total hydraulic loading rate.

Combining the data from the two years, as shown in Figure 14, suggests the trend toward production is related to the HLR rather than ammonium loading rate. For hydraulic loading rates less than 48 cm/d, scatter is approximately centered on zero removal regardless of ammonium loading rate while at the 59.7 cm/d HLR ammonium production averages 15 g/m^{2}d. This may lend credence to the sorption hypothesis as a confounding factor, higher hydraulic flow rates might flush more ammonium from sorption sites, increasing effluent mass relative to influent mass. However, a new steady-state would likely be reached shortly after the HLR increase, limiting the flushing effects.

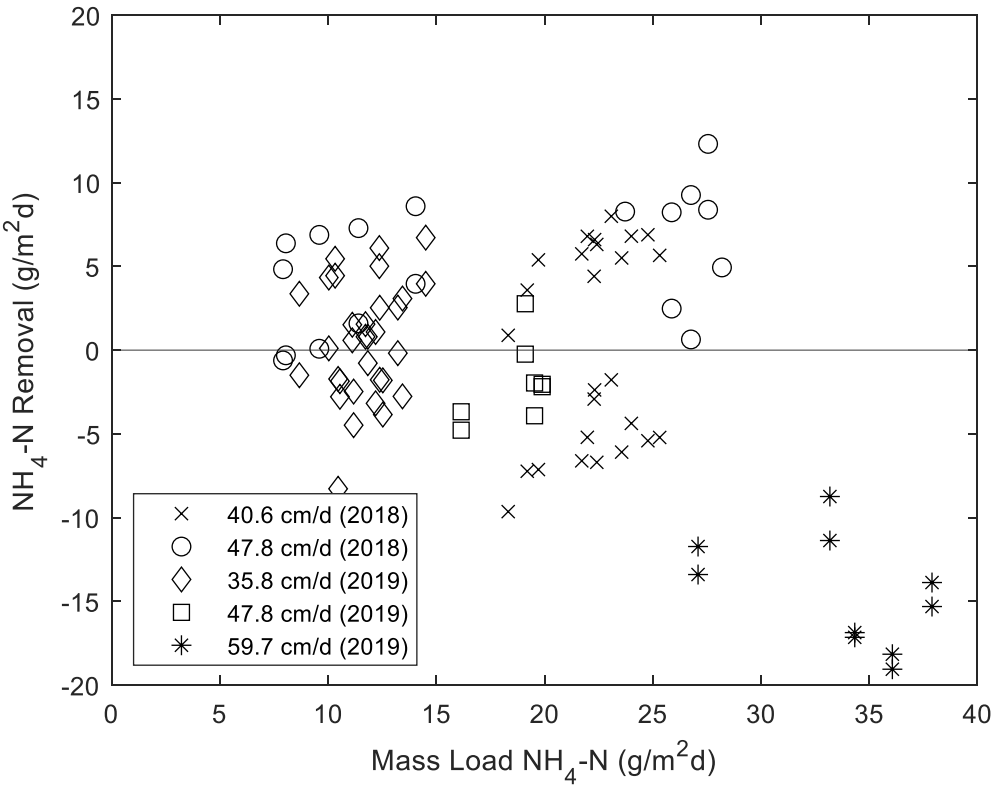

Figure 14. Mass removal of ammonium as a function of mass load of ammonium for the A cells in both system years 2018 and 2019, separated by total hydraulic loading rate.

Nitrate Mass Removal in the A Cells

A critical factor for total nitrogen removal is nitrate removal in the A cells. Mass removal of nitrate is plotted against the mass applied to the A cells for system year 2018 and 2019 in Figures 15-16, respectively. The data are only a partial representation of the denitrification process because nitrate potentially created in the upper aerobic layer is not only an unmeasured load to the saturated zone designed for denitrification but is also an unknown mass removed from the system.

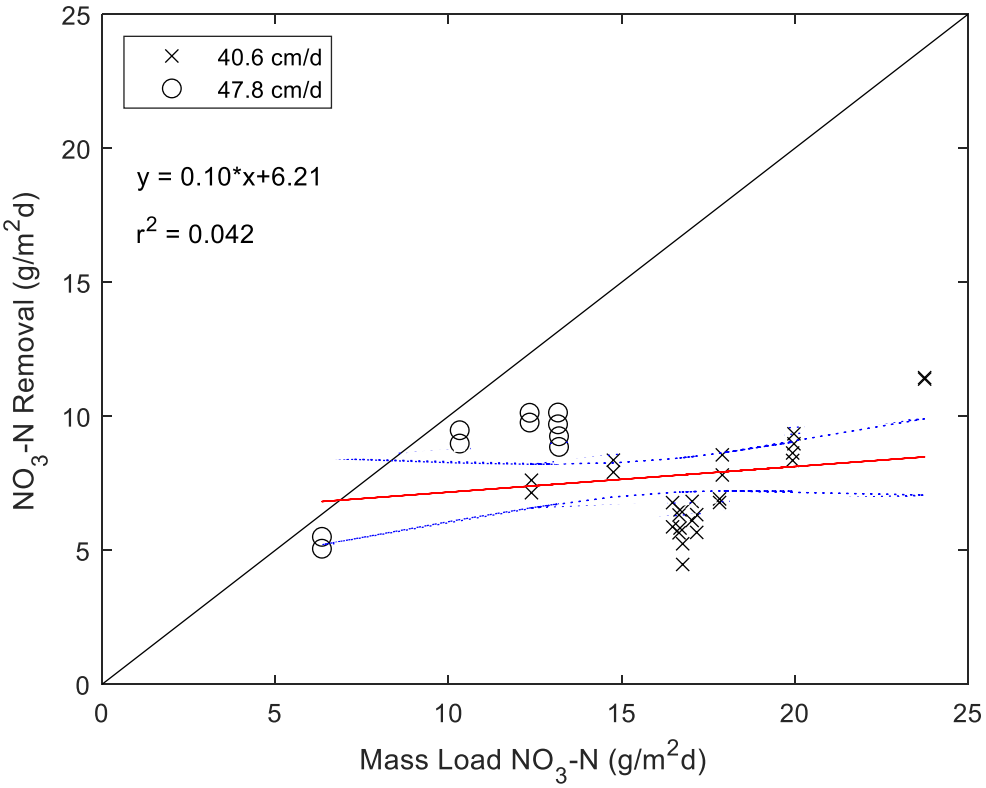

Figure 15. Mass removal of nitrate as a function of mass load of nitrate for the A cells in system year 2018, separated by total hydraulic loading rate. The 100% removal line is on the diagonal and a 95% confidence interval is the dotted line.

In 2018, applied nitrate loading to the A cells ranged from 6.3 g/m^{2}d to 24 g/m^{2}d. Nitrate concentrations in the transfer tank were high during the second half of this season (Fig. 3) which is reflected in the poor removal seen in Figure 15, especially at the 40.6 cm/d HLR. The relation between loading and removal is also poor, though a regression coefficient of 0.10 indicates that a small amount of denitrification occurred. These data can be immediately contrasted with nitrate removal from the A cells in 2019, shown in Figure 16.

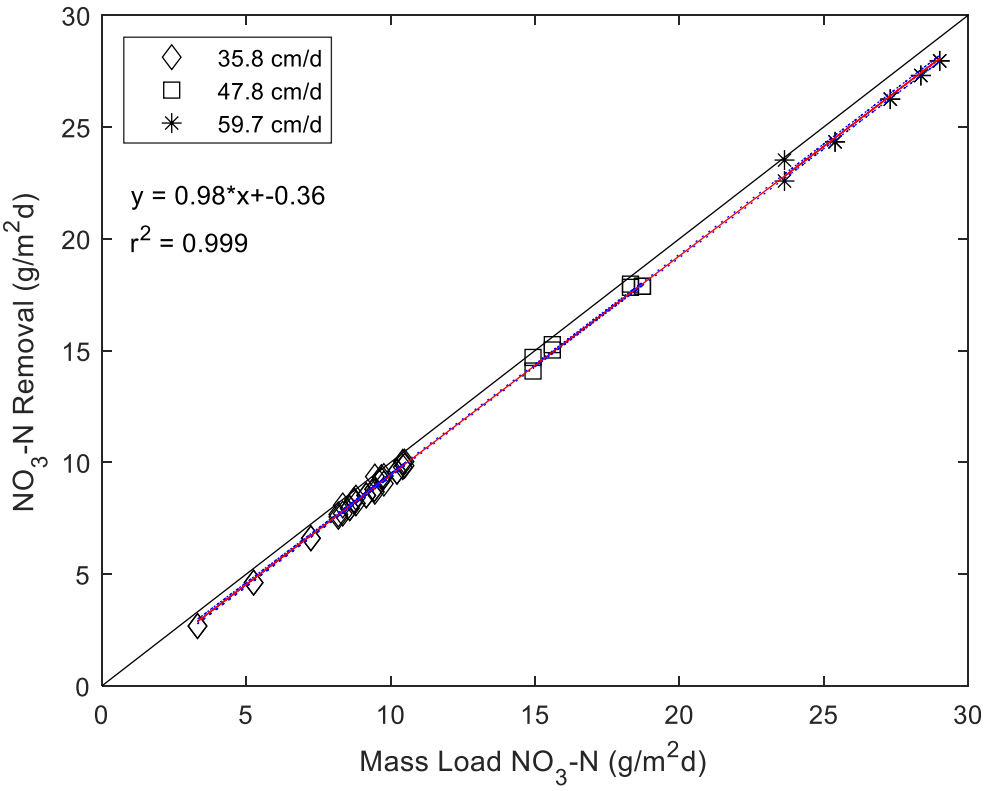

Figure 16. Mass removal of nitrate as a function of mass load of nitrate for the A cells in system year 2019, separated by total hydraulic loading rate. The 100% removal line is on the diagonal and a 95% confidence interval is the dotted line.

In 2019, nitrate loading to the A cells ranged from 3.3 g/m^{2}d to 29 g/m^{2}d. These results are highly linear, and a regression coefficient of 0.98 indicates that nearly 100% of nitrate applied to the A cells was removed, even at the highest HLR. To further clarify the contrast between denitrification in 2018 and 2019, A cell nitrate removal for both years is shown together in Figure 17.

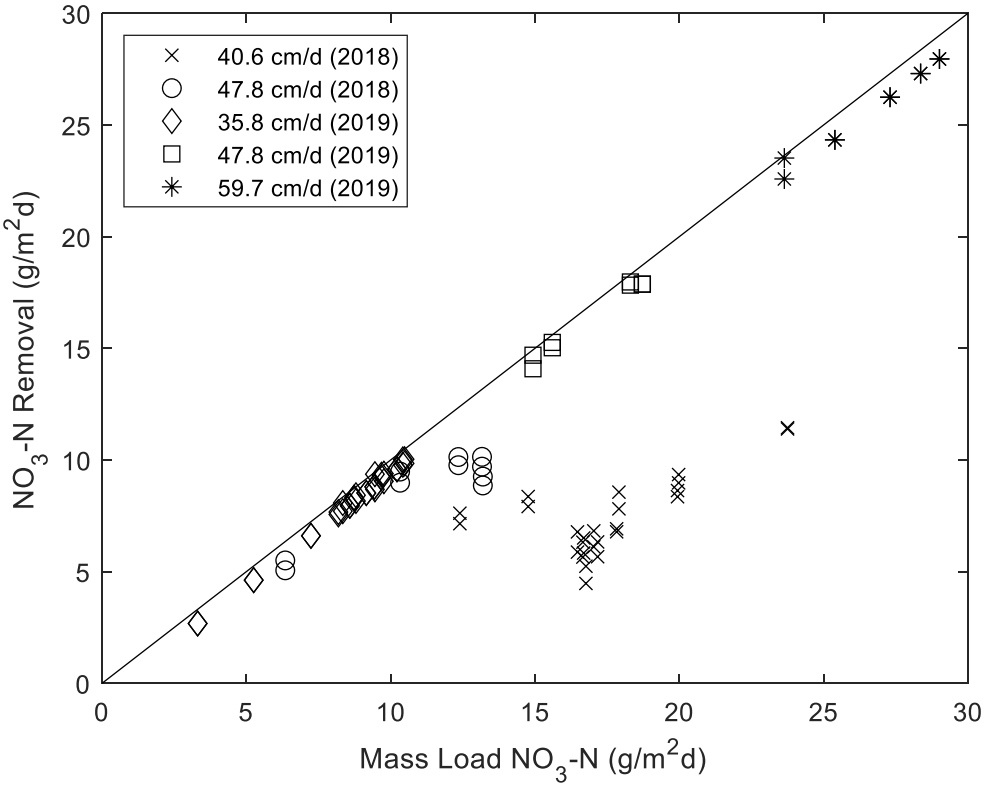

Figure 17. Mass removal of nitrate as a function of mass load of nitrate for the A cells in system years 2018 and 2019, separated by total hydraulic loading rate. The 100% removal line is on the diagonal.

Figure 17 clearly shows that, particularly at the 40.6 cm/d HLR, denitrification in 2018 was unexpectedly poor, with up to 12 g/m^{2}d of applied nitrate left untreated in the A cells. For comparison, the maximum amount of nitrate left untreated in 2019 was 1.1

g/m^2d. Clearly something disrupted the denitrification process during the second half of the season (see also Fig. 4) as poor performance is not correlated to either nitrate mass load or HLR. Additionally, it appears that the nitrate concentration in the transfer tank started to rise before the HLR was decreased from 47.8 to 40.6 cm/d (Figure 4). The most likely cause of this result is carbon limitation; the near-complete A cell COD removal seen in Figure 7 suggests that the system was likely limited by organic carbon during this period. Two other possible explanations are that the denitrification microbial community was somehow inhibited so that recycled nitrate was not denitrified or that the nitrification capability of the unsaturated zone was somehow enabled, converting a significant portion of the applied septic ammonium to nitrate, which then overwhelmed the denitrification capability within the saturation zone.

COD Removal in the B Cells

While the majority of COD removal should and did occur in the A cells (Figure 2), the system relies on the B cells to treat any COD that carries over. Some carryover is inevitable, but if excessive could limit B cell nitrification and subsequently denitrification (and COD removal) in the A cells. Thus, COD loading to the B cells not only influences its removal but might also be a marker for poor performance of the A cells. The mass removal of COD is plotted against mass load of COD to the B cells for system year 2018 in Figure 18.

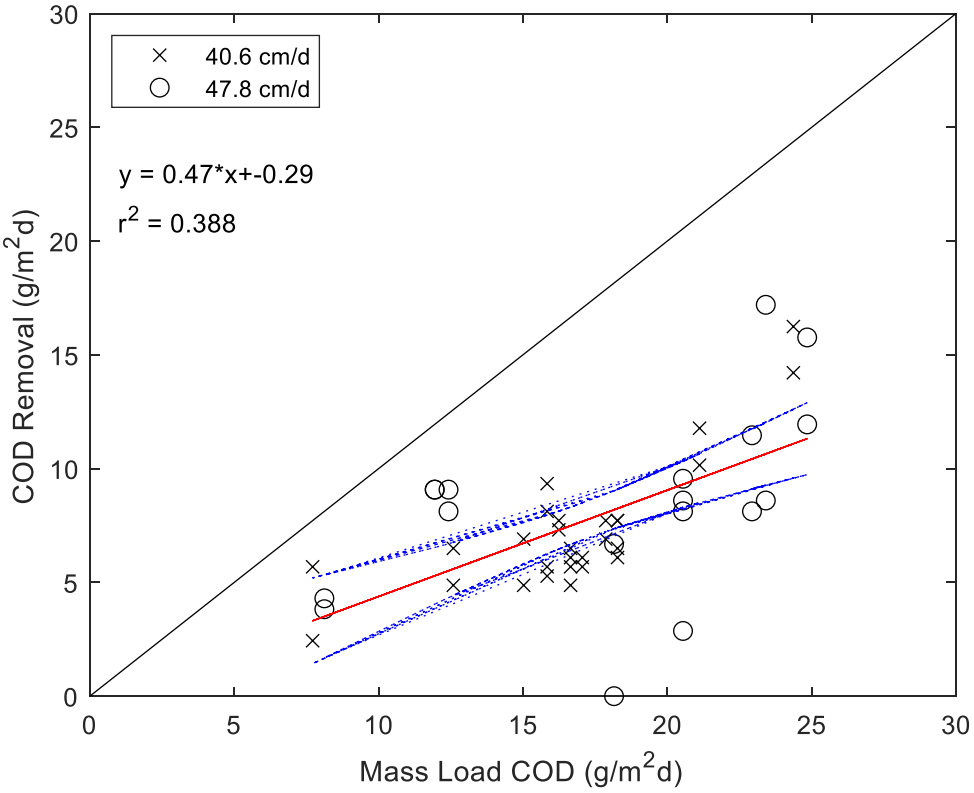

Figure 18. Mass removal of COD as a function of mass load of COD for the B cells in system year 2018, separated by total hydraulic loading rate. The 100% removal line is on the diagonal and a 95% confidence interval is the dotted line.

The mass load of COD to the B cells in 2018 ranged from 7.7 g/m^{2}d to 25 g/m^{2}d, roughly 10-20% of the loading to the A cells. In addition, this load would contain organics that are only slowly biodegradable because easily degraded organics would be removed in the A cells. Thus, a much lower regression coefficient 0.47 (versus 0.88 in the A cells) with more scatter (r^2 = 0.39) would be expected. As with the loading to the A cells, with the assumption that 25-30 mg/L of COD is non-biodegradable, the x-intercept should range between 10 and 15 g/m^{2}d. Given the lower mass loading of mostly non- and slowly-biodegradable COD, 47% removal is considered effective.

The mass removal of COD in the B cells is plotted similarly for system year 2019 in Figure 19. The mass load of COD to the B cells in 2019 ranged from 10 g/m^2d to 90 g/m^2d roughly 20-50% of the loading to the A cells. The largest mass loading of COD to the B cells for the 59.7 cm/d hydraulic loading rate corresponds to the decrease in removal effectiveness at that flow rate in the A cells (Figure 8). In this season, approximately 63% of the loaded COD was removed and showed a strong linearity with loading (r^2 of 0.94). Better removal than the previous year, especially at higher loading is expected; higher mass loadings include a larger fraction of biodegradable organics. An important practical result is that overall system COD removal was not affected by poor performance of the A cells.

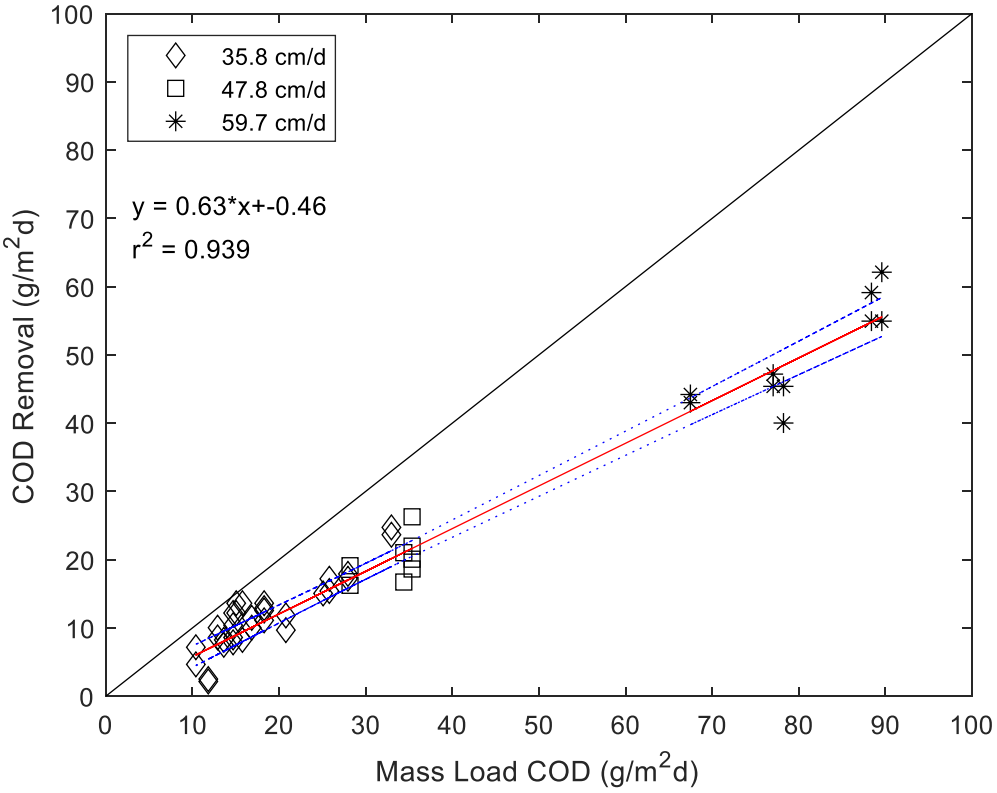

Figure 19. Mass removal of COD as a function of mass load of COD for the B cells in system year 2019, separated by total hydraulic loading rate. The 100% removal line is on the diagonal and a 95% confidence interval is the dotted line.

The B cells ability to remove carryover COD is further reinforced when mass removal of COD is plotted for system years 2017 through 2019 (Figure 20). Despite variation due to the season, COD loading, and hydraulic loading rate, COD removal in the B cells was consistent, with a combined regression coefficient of 0.64 and $r^2 = 0.91$. Compared to A cell performance, the lower coefficient suggests less efficient removal, but the performance decline is minimal and there appears to be no negative effect from the increased hydraulic loading rate. The lack of influence of HLR on performance is likely due to the smaller media size in the B cells; smaller pore space allows for more

water to be retained between dose loadings leading to longer residence times for biological activity.

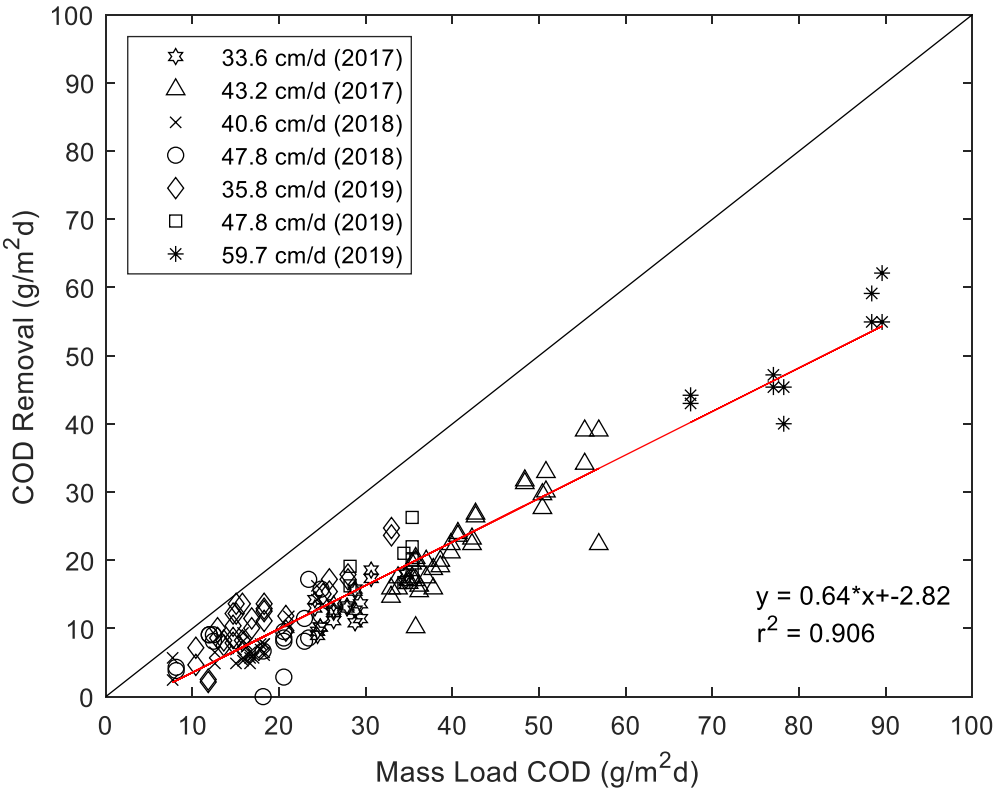

Figure 20. Mass removal of COD as a function of mass load of COD for the B cells for system years 2017 through 2019, separated by total hydraulic loading rate. The 100% removal line is on the diagonal. Data for 33.6 cm/d and 43.2 cm/d (2017) from Woodhouse (2018).

Ammonium Mass Removal in the B Cells

Finally, ammonium removal in the B cells must be considered, as this represents the effluent water quality for total nitrogen. Mass removal of ammonium is plotted against mass load of ammonium to the B cells for system year 2018 in Figure 21.

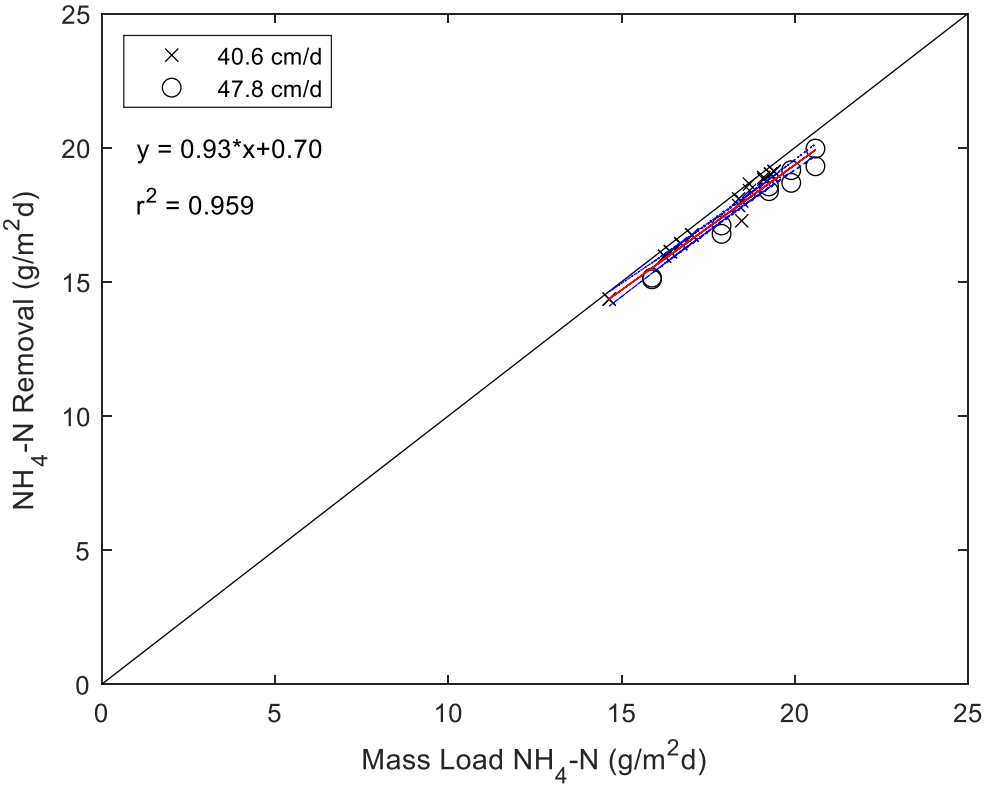

Figure 21. Mass removal of ammonium as a function of mass load of ammonium for the B cells in system year 2018, separated by total hydraulic loading rate. The 100% removal line is on the diagonal and a 95% confidence interval is the dotted line.

In 2018, ammonium loading to the B cells ranged from 15 g/m^{2}d to 21 g/m^{2}d. This is intrinsically related to A cell performance; ammonium not removed in the A cells is directly loaded onto the B cells. As the B cells are designed for nitrification, it is important to have a strong positive correlation between mass load and mass removal when assessing system performance for nitrogen removal. With a regression coefficient of 0.93, the B cells successfully transformed essentially all ammonium into nitrate at all ammonium mass loads and both HLR in 2018.

The mass removal of ammonium in the B cells is plotted similarly for system year 2019 in Figure 22. In 2019, ammonium loading to the B cells ranged from 5.3 g/m^{2}d to 54 g/m^{2}d. Note that a startup effect was observed in 2019, with poor ammonium removal at the first few sample events corresponding to the lowest mass loading rates and the 35.9 cm/d hydraulic loading rate. A regression analysis including all data points yields a regression coefficient of 0.78. It is immediately apparent that ammonium removal is further from the 100% removal line than in 2018. Ammonium removal of 78% is especially poor for the B cells, where near 100% removal is expected. However, removals at hydraulic loading rates of 35.8 cm/d and 47.8 cm/d still appear to be nearly 100%, only at the 59.7 cm/d hydraulic loading rate does performance seem to decline.

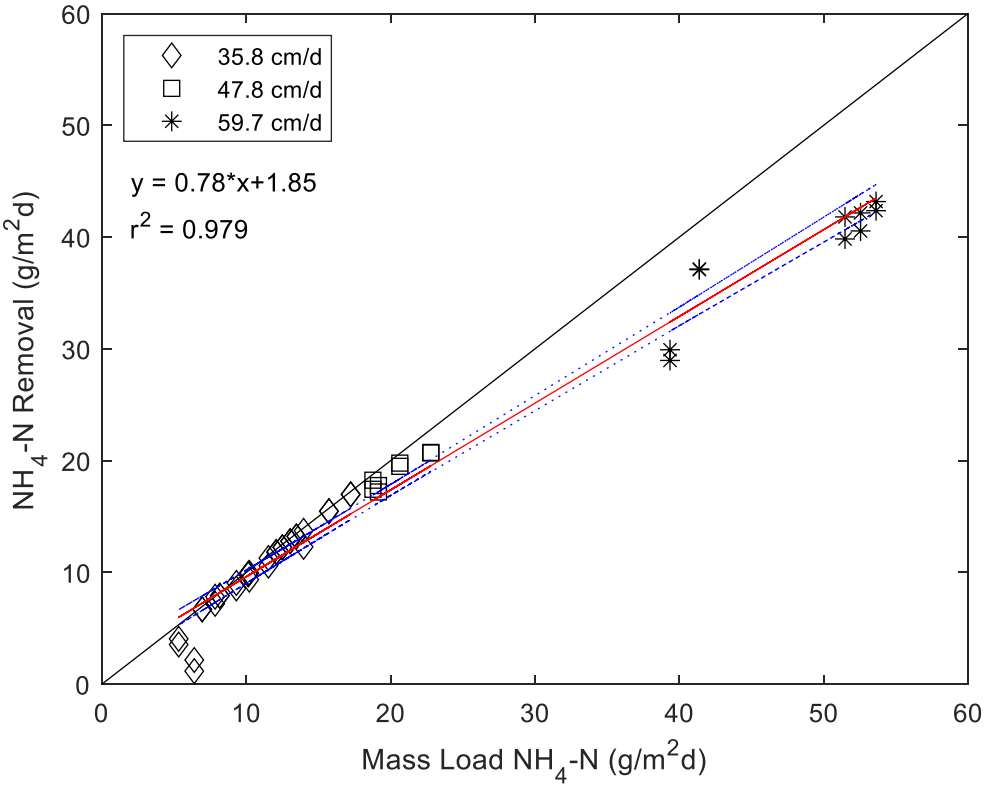

Figure 22. Mass removal of ammonium as a function of mass load of ammonium for the B cells in system year 2019, separated by total hydraulic loading rate. The 100% removal line is on the diagonal and a 95% confidence interval is the dotted line.

To further explore the performance decline at higher loading, ammonium removal is plotted for both system years 2018 and 2019 in Figure 23, with a linear regression that includes all hydraulic loading rates except 59.7 cm/d. As expected, removing the 59.7 cm/d data from the regression increases the regression coefficient to 1.02, larger than one partially due to inclusion of the startup data, effectively suggesting 100% removal within a small margin of error. Clearly, removal approaches 100% for mass loading rates up to about 25 g/m^{2}d or up to about 48 cm/d hydraulic loading rate, and is significantly less at loading rates above 40 g/m^{2}d corresponding to a hydraulic loading rate of 59.7 cm/d.

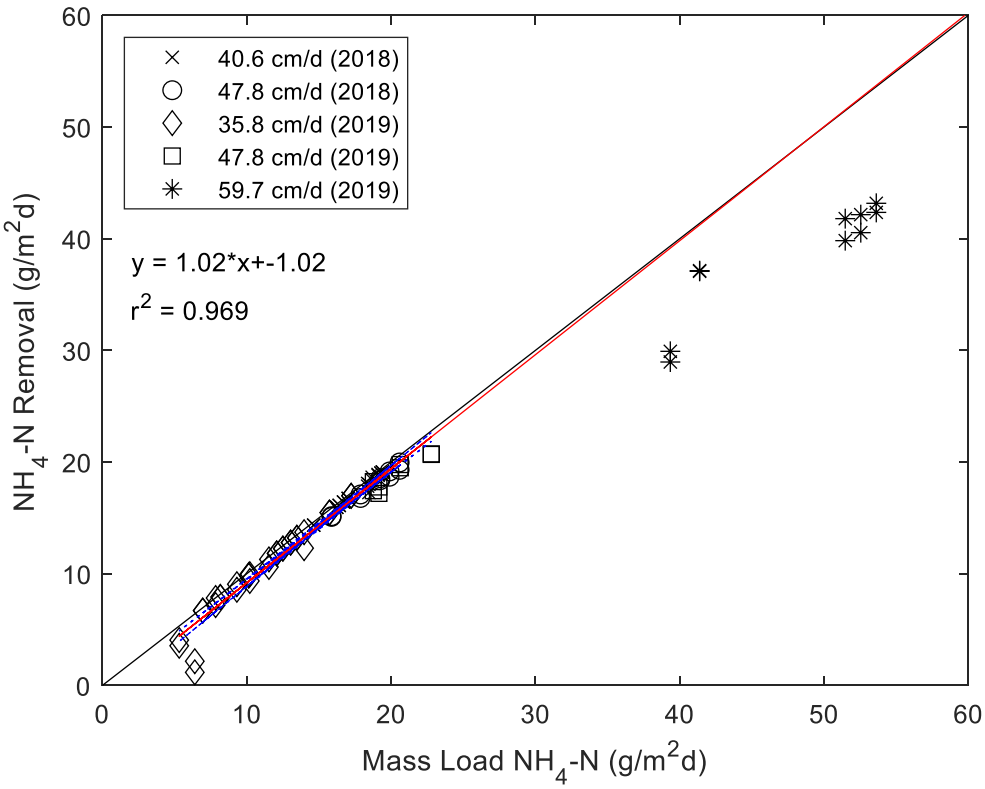

Figure 23. Mass removal of ammonium as a function of mass load of ammonium for the B cells in system years 2018 and 2019, separated by total hydraulic loading rate. The 100% removal line is on the diagonal and a 95% confidence interval is the dotted line.

One possible conclusion is that the poorer performance is related to either the higher mass ammonium load or the higher HLR, but the situation is more complicated. These higher loading rates also correspond to relatively poor performance of the A cells for COD removal (Figure 8) leading to much larger COD loading rates to the B cells, around 60-90 g/m^2d (Figure 19). This raises the possibility that nitrifier microbial activity was hampered by competition for oxygen with aerobic heterotrophs stimulated by the COD loading. This hypothesis is supported by the effective removal of COD in the B cells. In addition, poor nitrification in the B cells leads to much higher ammonium loading to the A cells (via recycle). While the ammonium load presented in Figures 15-17 considers both septic and recycle inputs to the A cells, the increased loading over multiple recycle doses perhaps influenced the apparent net ammonium production in the A cells at this loading rate. These observations highlight the interactions between different processes in the two stages of the system.

Multivariate B Cell Ammonium Removal

As previously explored, removal of COD and ammonium in the A cells and ammonium in the B cells decreased at the highest hydraulic loading rate of 59.7 cm/d. In the case of COD removal in the A cells the increased HLR at least partially explains the decreased performance, but the effects of mass loading of ammonium and COD cannot be separated from HLR in the cases of ammonium removal in the B cells. As a VFTW is a complex system with many interrelated components, it is beneficial to consider the combined effects of COD and ammonium on performance. Removal of carryover COD to the B cells is one possible explanation for poorer ammonium removal at the highest

HLR, because nitrifying bacteria are primarily chemotrophic, and COD can serve as a competing electron donor. This potentially affects all system processes by recycling increased ammonium and decreased nitrate loads to the A cells.

A multiple linear regression of ammonium removal in the B cells as predicted by combined COD loading and ammonium loading shows the individual effects of both components. The resulting model (mass loading basis) is as follows:

$$NH_4\ Removal = 2.12 + 0.96(NH_4\ Loading) - 0.12(COD\ Loading)$$

The regression coefficients for ammonium and COD loading are 0.96 and -0.12, respectively, and the intercept is 2.12. These coefficients are all significant at a 95% confidence level. The strong linear correlation (r^2 = 0.99) is visually represented in Figure 24, which plots ammonium removal predicted by the multiple linear regression against observed ammonium removals.

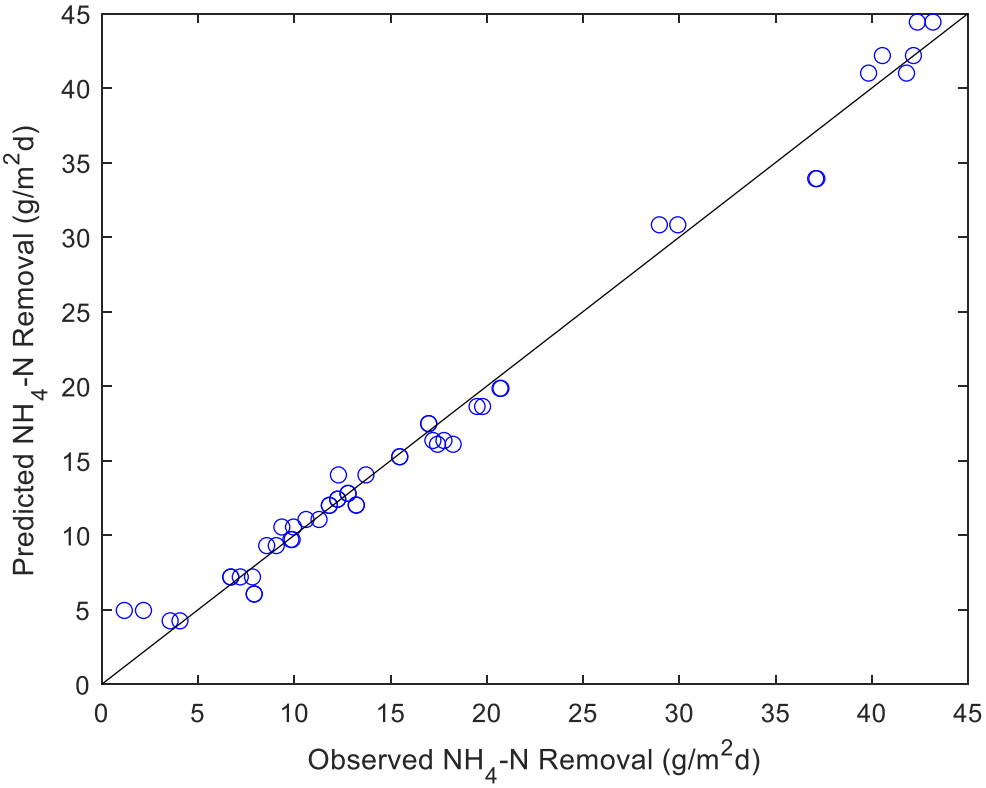

Figure 24. Predicted versus observed B cell ammonium removal from the multivariate linear regression model: $NH_4\ Removal = 2.12 + 0.96(NH_4\ Loading) - 0.12(COD\ Loading)$. A line representing a 1:1 ratio is on the diagonal.

Because the regression model including the negative influence of COD explains ammonium removal very effectively, the likely cause of the decreased ammonium removal at the 59.7 cm/d hydraulic loading rate is due to carryover of COD from the A cells rather than exceeding a maximum HLR or mass load of ammonium. A practical conclusion is that the A cells must remove most of the COD to have optimal nitrification in the B cells. Further, provided COD loads to the B cells remains low, the maximum HLR or ammonium load to the B cells has not been calibrated.

CONCLUSION AND RECOMMENDATIONS

The Bridger Bowl VFTW has continued to perform well for secondary wastewater treatment. Average removal was at least 96% of the applied ammonium and 95% of applied COD in system years 2018 and 2019 despite hydraulic loading rates higher than in previous years. TN removal was 67% and 54% for 2018 and 2019, respectively, indicating that the system, when operated with 2:1 recycle and 71 cm saturation of the first stage, was capable of significant denitrification. Overall, these results reinforce previous conclusions that VFTW systems are suitable for secondary wastewater treatment, even for relatively high-strength influent and in cold climates.

While seasonally averaged efficiencies remained high during this study, results suggest that there is an upper limit to the HLR beyond which a decrease in performance is observed. The upper limit appears to be between 47.8 cm/d and 59.7 cm/d, though this limit is likely influenced by other operational parameters including recycle ratio and saturation depth which were not varied during the study. At the highest hydraulic loading rate (59.7 cm/d) the mass removal of COD in the first stage and ammonium in the second stage deviates from a consistent trend with mass loading seen at lower HLRs. Ammonium removal in the second stage directly influences system performance and poorer nitrification in the second stage is the main reason average TN removal was lower in 2019 than 2018. Poorer COD removal in the first stage did not directly influence overall COD removal because the second stage was able to remove the carryover COD but is likely the main contributing factor to the reduced performance for ammonium removal in the second stage. This is evidenced by multivariate analysis of B cell ammonium removal considering ammonium and COD loading which shows that COD

loading onto the B cells inhibits ammonium removal. These results emphasize the interdependency of individual components of the system and that decreased performance of the first stage for COD removal will affect nitrification in the second stage.

Because influent concentrations were lower in 2018 and 2019 than in 2017, it was possible to infer that the reduction in COD removal within the first stage was more likely due to the increase in HLR rather than the increase in mass loading of COD. Nevertheless, the combined data set suggests that there is an upper limit for COD mass loading to the first stage as well. At COD loading rates higher than about 120 g/m^2d, COD removal tended to decline but was more apparent at higher HLR. As with an estimate for the maximum HLR, this maximum depends on the level of saturation of the first stage; no reduction in performance was observed for COD loading rates up to 160 g/m^2d when saturation level was only 53 cm (Woodhouse, 2018).

Consistent with prior results, nitrification in the second stage was nearly complete for ammonium loading rates up to about 25 g/m^2d corresponding to HLR up to 47.8 cm/d. However, performance declined (but still removed about 80% of the applied ammonium) for loading rates in the 40-55 g/m^2d corresponding to an HLR of 59.7 cm/d. As discussed above, poorer performance is likely due to the additional COD load to the second stage rather than the large HLR or ammonium loading, thus the capacity of the second stage to nitrify water without COD has not yet been determined.

Inferences on the effect of mass loading of nitrate onto the first stage (via recycle) on the denitrification process are confounded by unexplained poor performance during the second half of the 2018 season. Regardless, data from 2019 indicate nearly complete removal of applied nitrate up to 29 g/m^2d corresponding to the 59.7 cm/d HLR. Since the

denitrification zone is saturated, the maximum HLR for denitrification is likely larger than processes dependent on unsaturated zones.

The HLRs used in the analysis represent the total load including that from the septic tank and the recycle tank thus a different recycle ratio would change the HLR while having minimal influence on mass loading rates. Though Woodhouse (2018) determined overall treatment effectiveness was best at 2:1 recycle and 71 cm saturation of the first stage and these settings were used in this study, better understanding of the effect of HLR might allow a revisit of optimal settings of these two parameters. The dose schedule is another operational variable influencing performance and it is possible that a different dose schedule could increase the maximum loadings determined in this study. One option would be to consider high HLRs but with more frequent small doses as this might minimize ammonia desorption or increase aerobic respiration for COD removal in the first stage. Optimizing for complete removal of COD in the first stage maximizes the nitrification potential of the second stage. As the first and second stage cell pairs are now established as replicates, they could be run using different schemes in parallel to strengthen conclusions about hydraulic loading effects as well. Otherwise, the upper limit for the treatment effectiveness of the system has yet to be found, and simply continuing the methodology of this study at higher HLR may clarify some results.

Finally, it is noteworthy that construction of an identically designed, scaled-up VFTW is now complete adjacent to the experimental system studied herein. With access to water quality from this system, potentially groundbreaking results about VFTW scale-up could be made. For this to be most effective, the two systems would need to be operated identically. This is another possible benefit of running the A and B cells

separately, as one of each cell could be run to match the full-scale system, while the other could undergo experiments that have a higher risk of decreasing overall treatment effectiveness.

REFERENCES CITED

Allen, C. R.; Stein, O. R.; Hook. P. B.; Burr. M. D.; Parker, A. E.; Hafla, E. C. "Temperature, Plant Species and Residence Time Effects on Nitrogen Removal in Model Treatment Wetlands." *Water Science and Technology*, vol. 68, no. 11, 2013, pp. 2337–2343., doi:10.2166/wst.2013.482.

Almeida, A.; Carvalho, F.; Imaginário, M.J.; Castanheira, I.; Prazeres, A.R.; Ribeiro, C. "Nitrate Removal in Vertical Flow Constructed Wetland Planted with Vetiveria Zizanioides: Effect of Hydraulic Load." *Ecological Engineering*, vol. 99, 2017, pp. 535–542., doi:10.1016/j.ecoleng.2016.11.069.

Arias, C.A.; Brix, H.; Marti, E. "Recycling of Treated Effluents Enhances Removal of Total Nitrogen in Vertical Flow Constructed Wetlands." *Journal of Environmental Science and Health, Part A*, vol. 40, no. 6-7, 2005, pp. 1431–1443., doi:10.1081/ese-200055882.

Croghan, C. W., & Egeghy, P. P. Methods of Dealing with Values Below the Limit of Detection using SAS. Retrieved from Las Vegas, NV.

Dotro, G.; Langergraber, G.; Molle, P.; Nivala, J.; Puigagut, J.; Stein, O.; von Sperling, M. (2017). *Treatment Wetlands* (Biological Wastewater Treatment Series Vol. 7). London: IWA.

USEPA. (1982). Handbook for Sampling and Sample Preservation of Water and Wastewater. Cincinnati, Ohio.

Hanson, A.M., and G.F. Lee. "Forms of Organic Nitrogen in Domestic Wastewater." *Water Pollution Control Federation*, Nov. 1971.

Kadlec, Robert H., and Scott D. Wallace. *Treatment Wetlands*. CRC Press, 2009.

Langergraber, G.; Pressl, A.; Leroch, K.; Rohrhofer, R.; Haberl, R. "Comparison of Single-Stage and a Two-Stage Vertical Flow Constructed Wetland Systems for Different Load Scenarios." *Water Science and Technology*, vol. 61, no. 5, 2010, pp. 1341–1348., doi:10.2166/wst.2010.024.

Lee, C.; Fletcher, T.D.; Sun, G. "Nitrogen Removal in Constructed Wetland Systems." *Engineering in Life Sciences*, vol. 9, no. 1, 2009, pp. 11–22., doi:10.1002/elsc.200800049.

Lin, Y.; Jing, S.; Lee, D.; Chang, Y.; Shih, K. "Nitrate Removal from Groundwater Using Constructed Wetlands under Various Hydraulic Loading Rates." *Bioresource Technology*, vol. 99, no. 16, 2008, pp. 7504–7513., doi:10.1016/j.biortech.2008.02.017.

Liu, Guoqiang, and Jianmin Wang. "Enhanced Removal of Total Nitrogen and Total Phosphorus by Applying Intermittent Aeration to the Modified Ludzack-Ettinger (MLE) Process." *Journal of Cleaner Production*, vol. 166, 2017, pp. 163–171., doi:10.1016/j.jclepro.2017.08.017.

Luederitz, V.; Eckert, E.; Lange-Weber, M.; Lange, A.; Gersberg, R.M. "Nutrient Removal Efficiency and Resource Economics of Vertical Flow and Horizontal Flow Constructed Wetlands." *Ecological Engineering*, vol. 18, no. 2, 2001, pp. 157–171., doi:10.1016/s0925-8574(01)00075-1.

Molle, P.; Prost-Boucle, S.; Lienard, A. "Potential for Total Nitrogen Removal by Combining Vertical Flow and Horizontal Flow Constructed Wetlands: A Full-Scale Experiment Study." *Ecological Engineering*, vol. 34, no. 1, 2008, pp. 23–29., doi:10.1016/j.ecoleng.2008.05.016.

Morvannou, A,; Chouber, J.; Vanclooster, M.; Molle, P. "Modeling Nitrogen Removal in a Vertical Flow Constructed Wetland Treating Directly Domestic Wastewater." *Ecological Engineering*, vol. 70, 2014, pp. 379–386., doi:10.1016/j.ecoleng.2014.06.034.

Moss, J. J. (2016). Operation and Optimization of a Two-Stage, Vertical Flow Constructed Wetland System at Bridger Bowl Ski Area. (Environmental Engineering), Montana State University, Bozeman, MT.

Paing, J.; Guilbert, A.; Gagnon, V.; Chazarenc, F. "Effect of Climate, Wastewater Composition, Loading Rates, System Age and Design on Performances of French Vertical Flow Constructed Wetlands: A Survey Based on 169 Full Scale Systems." *Ecological Engineering*, vol. 80, 2015, pp. 46–52., doi:10.1016/j.ecoleng.2014.10.029.

Saeed, Tanveer, and Guangzhi Sun. "A Review on Nitrogen and Organics Removal Mechanisms in Subsurface Flow Constructed Wetlands: Dependency on Environmental Parameters, Operating Conditions and Supporting Media." *Journal of Environmental Management*, vol. 112, 2012, pp. 429–448., doi:10.1016/j.jenvman.2012.08.011.

Stefanakis, Alexandros I. "Constructed Wetlands." *Practice, Progress, and Proficiency in Sustainability Impact of Water Pollution on Human Health and Environmental Sustainability*, pp. 281–303., doi:10.4018/978-1-4666-9559-7.ch012.

Stefanakis, Alexandros I., and Vassilios A. Tsihrintzis. “Effects of Loading, Resting Period, Temperature, Porous Media, Vegetation and Aeration on Performance of Pilot-Scale Vertical Flow Constructed Wetlands.” *Chemical Engineering Journal*, vol. 181-182, 2012, pp. 416–430., doi:10.1016/j.cej.2011.11.108.

Taylor, C. R., Hook, P. B., Stein, O. R., & Zabinski, C. A. (2010). Seasonal effects of 19 plant species on COD removal in subsurface treatment wetland microcosms Ecological Engineering, 37, 703-710. doi:10.1016/j.ecoleng.2010.05.00

Vymazal, Jan, and Lenka Kröpfelová. “Multistage Hybrid Constructed Wetland for Enhanced Removal of Nitrogen.” *Ecological Engineering*, vol. 84, 2015, pp. 202–208., doi:10.1016/j.ecoleng.2015.09.017.

Vymazal, Jan. “Horizontal Sub-Surface Flow and Hybrid Constructed Wetlands Systems for Wastewater Treatment.” *Ecological Engineering*, vol. 25, no. 5, 2005, pp. 478–490., doi:10.1016/j.ecoleng.2005.07.010.

Vymazal, Jan. “Removal of Nutrients in Various Types of Constructed Wetlands.” *Science of The Total Environment*, vol. 380, no. 1-3, 2007, pp. 48–65., doi:10.1016/j.scitotenv.2006.09.014.

“Wastewater Treatment by Tropical Plants in Vertical-Flow Constructed Wetlands.” *Water Science and Technology*, vol. 40, no. 3, 1999, doi:10.1016/s0273-1223(99)00462-x.

Woodhouse, S. L. (2018). Influence of Saturation on Denitrification in a Two-Stage, Vertical Flow Treatment Wetland at Bridger Bowl Ski Area. (Environmental Engineering), Montana State University, Bozeman, MT.